Reclus, a new Database for Investigating the Tectonics of the Earth: an Example from the East African Margin and Hinterland

Paul Markwick[1], Douglas Paton[2], and Estelle Mortimer[3]

[1]Knowing Earth Limited
[2]TectonKnow Limited
[3]University of Leeds

November 22, 2022

Abstract

The open availability of global scientific databases is key to advancing research of the Earth system and facilitating cross-disciplinary studies. There are numerous datasets available for investigating tectonics, but none that provide an internally consistent representation of the structural framework, crustal architecture, and geodynamics. We present Reclus, a suite of global, integrated databases that fill this gap, thereby providing the community with the key components for investigating the Earth system. Reclus includes databases of the following: (1) structural elements, which define the three-dimensional geometry of the rock volume, including folds and faults; (2) 'crustal' facies describing the geometry and composition/rheology of the lithosphere; (3) igneous features; and (4) geodynamics, representing the dominant thermo-mechanical processes acting on the lithosphere. These databases and workflows are applied to East Africa to investigate the geometry and heterogeneity of the margin and its hinterland. This margin is often summarised in the literature as a 'transform margin,' represented by a single structural feature, the 'Davie Fracture Zone', but it is much more complicated. We show how the pre-existing structure, the superimposition of successive tectonic cycles, and crustal heterogeneity dictate the complexity observed.

Reclus, a new Database for Investigating the Tectonics of the Earth: an Example from the East African Margin and Hinterland

P. J. Markwick[1,3], D. A. Paton[2], and E. J. Mortimer[3]

[1] Knowing Earth Limited, West Yorkshire, U.K.

[2] TectonKnow Limited, West Yorkshire, U.K

[3] School of Earth and Environment, University of Leeds, Leeds, West Yorkshire, U.K.

Corresponding author: Paul Markwick (paul,markwick@knowing.earth)

Key Points:

- The open availability of global databases is key to advancing research of the Earth System
- We present a new high-resolution suite of baseline databases for investigating tectonics
- The databases provide a systematic way to identify uncertainty and data gaps and pose new hypotheses for further, more detailed research.

Abstract

The open availability of global scientific databases is key to advancing research of the Earth system and facilitating cross-disciplinary studies. There are numerous datasets available for investigating tectonics, but none that provide an internally consistent representation of the structural framework, crustal architecture, and geodynamics. We present Reclus, a suite of global, integrated databases that fill this gap, thereby providing the community with the key components for investigating the Earth system. Reclus includes databases of the following: (1) structural elements, which define the three-dimensional geometry of the rock volume, including folds and faults; (2) 'crustal' facies describing the geometry and composition/rheology of the lithosphere; (3) igneous features; and (4) geodynamics, representing the dominant thermo-mechanical processes acting on the lithosphere. These databases and workflows are applied to East Africa to investigate the geometry and heterogeneity of the margin and its hinterland. This margin is often summarised in the literature as a 'transform margin,' represented by a single structural feature, the ‘Davie Fracture Zone’, but it is much more complicated. We show how the pre-existing structure, the superimposition of successive tectonic cycles, and crustal heterogeneity dictate the complexity observed.

Plain Language Summary

Scientific databases are important for developing and testing ideas. For studying plate tectonics, there are a large number of databases available. But, absent from this list are detailed, global databases that link interpretations of faults and folds with the distribution of different crustal compositions and thicknesses. These databases are important because these features dictate how the crust responds to tectonic forces, which may result in changes in where sediments are deposited, new folding and faulting, and uplift or subsidence. We have built a suite of databases, collectively called *Reclus*, that fills this gap. These are spatial databases interpreted primarily from remote sensing and seismic data. They are supported by a comprehensive audit trail that explains what the interpretations are based on and how confident a researcher can be in using them. These databases are designed to provide a baseline resource for the scientific community

with which we can test hypotheses, look at large-scale patterns, and identify where new data and research is needed.

1 Introduction

Observational data are fundamental to scientific advancement. Recently many governments and research bodies have made their data, and the data obtained through their funding, open to the public. This has proved invaluable for furthering our understanding of the Earth system. Primary data, including Landsat imagery (NASA Landsat Program, 2000), radar (SRTM: Shuttle Radar Topography Mission), and the results of the DSDP and ODP drilling programs, provided by the U.S. Government are amongst the most important contributions to Earth sciences available. Other countries, notably Australia, Canada, New Zealand, and Norway, make industry acquired potential fields, seismic and well data available after a specified duration of time. For tectonics, there are a range of digital datasets now available, including the following: plate models (Seton et al., 2012); plate polygons (Bird, 2003); sedimentary basins (CGG Robertson, 2020; USGS World Energy Assessment Team, 2000); hotspots (Whittaker et al., 2013); isochrons (Müller et al., 1997; Royer et al., 1992); ocean age (Müller et al., 2008); ocean fabric (Gahagan et al., 1988; Royer et al., 1989); large igneous provinces (Coffin and Eldholm, 1994); crustal thickness (Mooney et al., 1998); stress (Heidbach et al., 2018); thermo-tectonic age (USGS, https://earthquake.usgs.gov/data/crust/maps.php); seamounts (Kim and Wessel, 2011; Wessel, 1997); earthquakes (USGS, 2019); and volcanoes (Global Volcanism Program, 2019; Simkin and Siebert, 1994).

Absent from this list are detailed global databases of structural elements, crustal composition and geometry, and geodynamics. But these are fundamental in constraining plate models, defining basin form (basin dynamics), and understanding the development and distribution of accommodation space and heat flow (a key input in both maturity modeling in petroleum exploration and geothermal exploration). The interplay between geodynamics and crustal architecture dictates landscape evolution, and therefore paleogeography and source-to-sink. It is upon the resulting landscape that the geological record is built. Many major transport

pathways (rivers and submarine cantons) are structurally defined, for example, the Benue River through the Benue Trough, the Zambezi Rover via the Middle and Lower Zambezi basins, the Amazon River along the Amazonas shear zone, and Lurio Rivers in East Africa.

The notion of a database and maps depicting crustal architecture predates plate tectonic theory, for example, Boué's global map of "geological structure" (published in Johnston, 1856) or Reclus' (1876) global maps of volcanoes and mountain belts. Reference to the "architecture of the crust" was first made by Hunt (1873), who saw it as key to interpreting the geological record by underpinning what he called "paleogeographic maps" - reconstructions of the surface of the Earth through time. This was a view supported by subsequent paleogeographers (Schuchert, 1910; 1928; Ziegler et al., 1985).

With the advent of plate tectonics in the late 1960s, the need for up-to-date global maps resulted in Exxon's "Tectonic map of the world" (Exxon Production Research Company, 1985), showing the distribution of major structural elements, basins, isopachs, and basement. Subsequently, published datasets included the compilations of the CGMW (2010) and Bally et al., (2012). Yet, the representation of the crustal architecture and structural elements on these maps is still quite generalized. More detailed maps are available, for example, the DOTSEA and DOTMED databases (Chamot-Rooke et al., 2005; Pubellier et al., 2005), but these are geographically limited and lack a comprehensive attribution and audit trail.

This study aims to construct and make openly available a baseline suite of databases that can be used by the community to further our understanding of the Earth system. We have called this suite Reclus, after the French geographer Jacques Élisée Reclus", whose 19 volume work, La Nouvelle Géographie Universelle, la Terre et Les Hommes, examined the physical and human geography of every continent, including some of the first maps illustrating the global distribution of volcanoes and mountains. Reclus has been designed to enable cross-disciplinary integration and use in analyses including the following: geodynamic modeling; plate reconstructions; structural analysis; paleogeography; paleobiogeography; paleoecology: source-to-sink analysis; paleoclimatology and Earth system modeling. To achieve this is fully integrated across its components, reflecting the close interplay of each element in the Earth system.

Reclus differs from existing databases in the following ways: (1) it includes a consistent representation of global crustal types, especially along passive margins where this is required for

a broad application in restoration modeling, heat flow modeling, and plate tectonic restoration; (2) a more detailed and consistent structural elements database; (3) a geodynamics component that explicitly records the time since the last thermo-mechanical event to affect any part of the crust; (4) it forms part of a more comprehensive, integrated workflow developed to build paleogeographic maps and paleolandscapes as the backdrop for understanding the Earth system (Markwick, 2019).

The problem of representing and classifying the structural framework and crustal architecture is exacerbated in geographic areas such as East Africa, where multiple tectonic cycles have resulted in a complex, superimposed history that dictates how the margin and hinterland develop (Macgregor, 2015; Reeves, 2017; Reeves et al., 2016). This complexity makes it an ideal test of the utility of the Reclus baseline databases and workflows. This includes their application in resource exploration, geohazard, and environmental studies. East Africa is an area of on-going exploration for oil and gas (Brownfield, 2016), minerals, metals, and geothermal energy (Delvaux et al., 2010; Kraml et al., 2014; Martinelli et al., 1995; Mnjokava, 2012). The Durban Basin offshore SE Africa is the site of investigations for carbon storage (Hicks and Green, 2017).

Figure 1 shows the study area used in this paper. From this area we develop three examples to illustrate how these databases provide a systematic baseline with which to understand the regional context of detailed studies and how our interpretations compare and contrast with existing interpretations:

1. The Davie Deformational Zone (DDZ)
2. The interplay of pre-existing fabrics.
3. The Biera High and Mozambique Lowlands

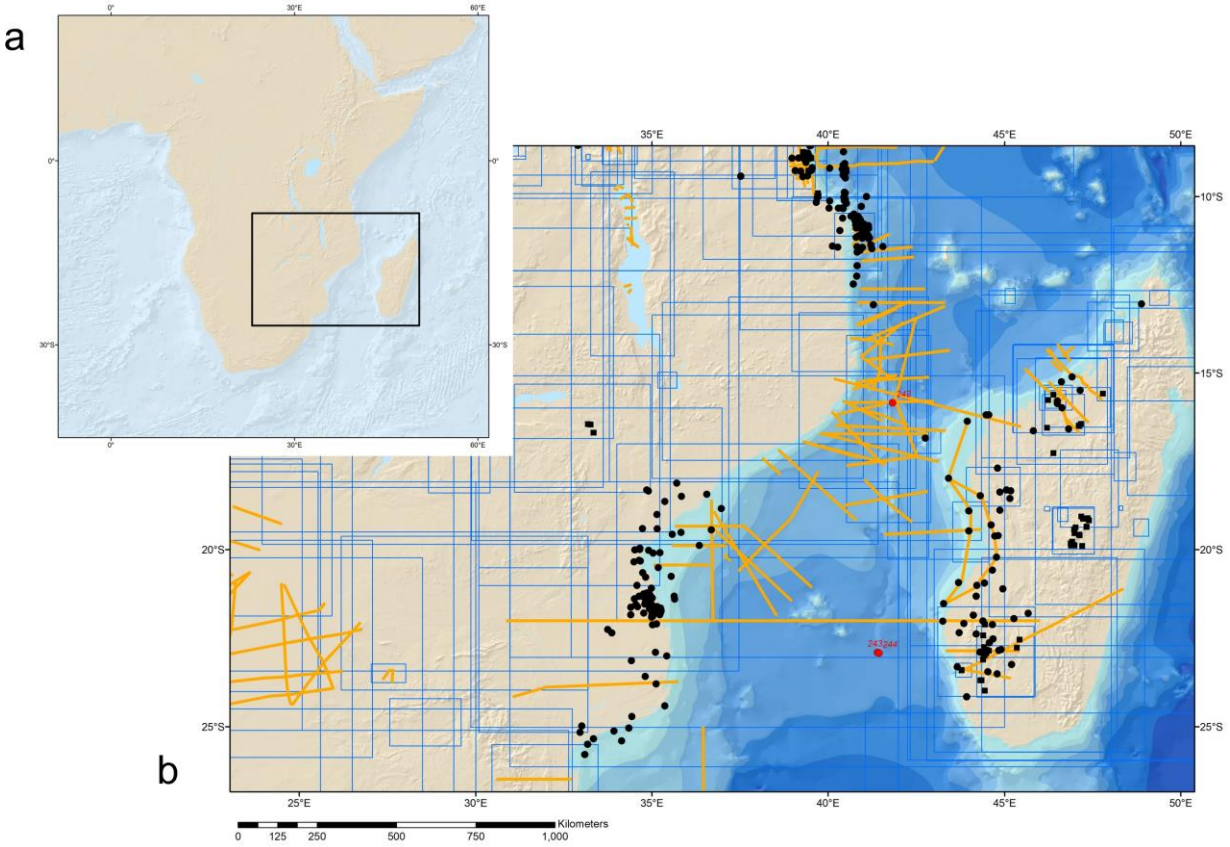

Figure 1. **a**, Location map showing extent (black box) used as the example in this study. **b**, The distribution of published seismic lines (orange lines), wells (black filled circles), and reference footprints (blue outlines) used to constrain the databases. This is in addition to the other primary datasets described in the text, including potential fields data, radar, Landsat and seismicity.

2 Materials and Methods

The *Reclus* databases have been designed, compiled, and managed using ESRI's ArcGIS software (ESRI, 2017). They are underpinned by a comprehensive data management system and systematic attribution; details are included in Supporting Information (S.I.). The availability of such a comprehensive audit and attribution are key if the data are to be used and improved upon, especially when used as input to AI (Artificial Intelligence) systems.

146

147

148 ## 2.1 Workflow

149 The workflow used to generate the databases is based upon that described in Markwick
150 (2019) and is summarised in Figure 2. We present a summary of each database, including the
151 input data, below and provide full methodology and details within S.I.

152

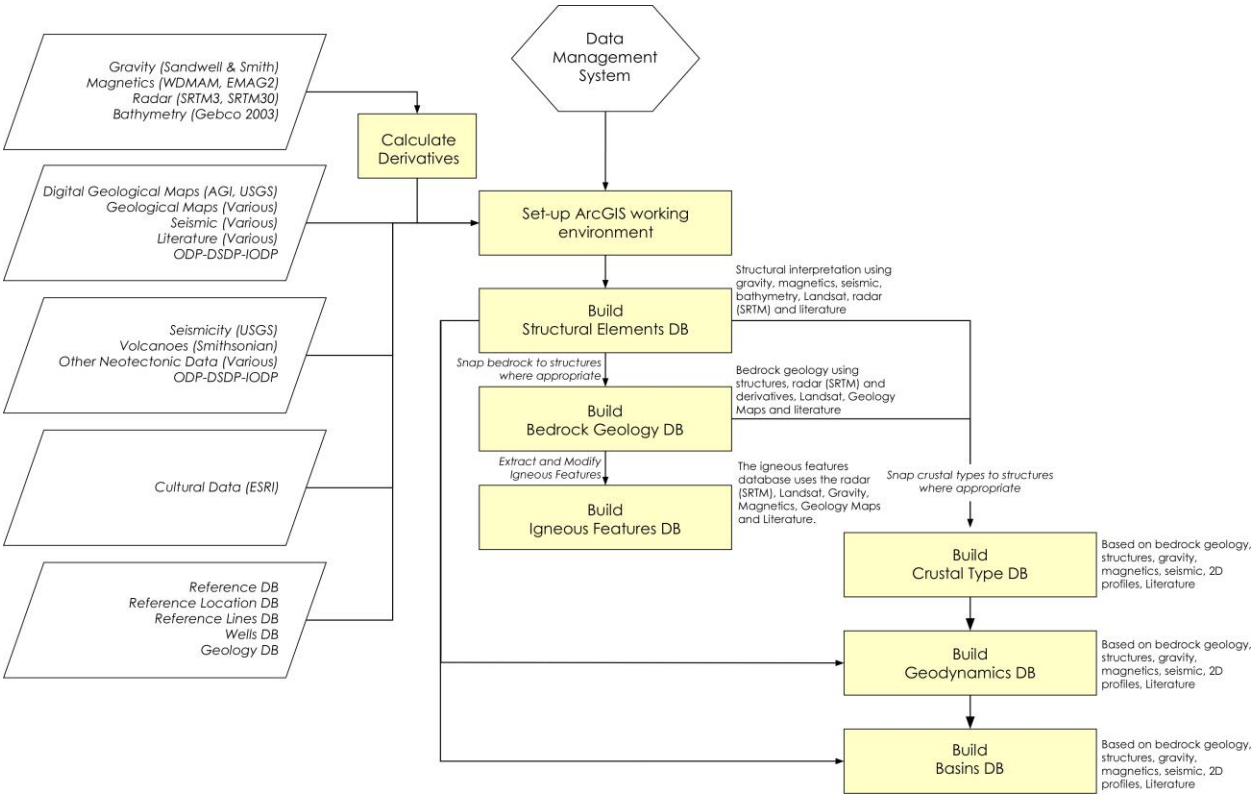

153

154

155 **Figure 2**. The high-level workflow used for building the databases described in this study.

156

157 ## 2.2 Definitions

158 The terminology associated with published tectonics studies is commonly, but often
159 inconsistently, used. We, therefore, provide explicit definitions of our usage (Table 1).

160

161

162 **Table 1.** Definitions of the key terms used throughout this paper.

163

Term	Definition	Notes
Crustal architecture	The geometry (spatial extent and thickness), character (composition and rheology), and structural framework of the Earth's lithosphere.	Crustal architecture is the product of past geodynamic processes, but in turn, dictates how the crust responds to subsequent geodynamics resulting from changes in the tectonic regime. The term was originally coined by Thomas Sterry Hunt in 1873 ("T*he structure and arrangement of the materials of the earth's crust, its architecture, as it were" p.416*).
Structural framework	The three-dimensional geometry of the rock record as the product of deformation and therefore the record of the strain applied to the rock volume.	This deformation is the response of the existing crustal architecture to geodynamic forcing. The structural framework is an integral part of the crustal architecture, but in most usage referred to separately.
Geodynamics	The dynamic processes that shape the Earth. These comprise the dominantly horizontal stresses resulting from and leading to the motion of tectonic plates, and the dominantly vertical stresses resulting from mantle processes and, locally, igneous activity.	The direct consequence of geodynamics is deformation, the product of which is the revised crustal architecture with the specific deformational activity recorded by the structural framework. How the Earth responds to geodynamic forcing's will vary depending on the stresses involved and the pre-existing crustal architecture.
Tectonics	The description of the processes that 'build' the Earth's crust and define its evolution through time.	The term 'tectonics' encompasses both crustal architecture and geodynamics and is explicitly linked with the concept of plate tectonics, especially the largely horizontal plate motions that drive and result from horizontal stresses. As such tectonics, like crustal architecture, considers more than just the crust, and needs to include an understanding of the Earth's lithosphere and mantle processes.

164

165 ### 2.3 Input Data

166 The primary datasets used in this study include published satellite gravity (Sandwell and
167 Smith, 2009; Sandwell et al., 2014), magnetics (Lesur et al., 2016; Maus et al., 2007; Maus et al.,
168 2009), radar (Farr et al., 2007), Landsat (NASA Landsat Program, 2000) and published well and
169 seismic data (Figure 1). More detailed field-based gravity data, including FTG surveys, and
170 aeromagnetic data, have been used where these are published. The bathymetric dataset employed
171 is that of Gebco (IOC et al., 2003) as this was the last version to be based on soundings without
172 including bathymetric interpretations from gravity inversion. Secondary data (published

interpretations from other researchers) are used to provide information on the geological significance of features, including age, kinematics, petrology, depositional environments.

2.4 Scale and resolution, confidence and precision

For digital spatial databases, the term "scale" is problematic because the same information can be represented at any 'scale' whatever its original compilation scale and intended purpose.

Markwick and Lupia (2002) described the importance of scale and resolution in geological problem solving and recommended the use of the term "resolution" rather than "scale" in describing spatial data. They adopted the concept of the "minimal resolvable feature" resolution (Tobler, 1988) as a useful way of indicating spatial limitations. Each input dataset used in our interpretations has its intrinsic grain (the grain is the minimum resolution of an observation or data; the smallest spatial or temporal interval of observation) and coverage density, which can vary with depth and geographical location depending on the capture methods (viz., the grain of magnetic data coarsens with the depth to the magnetic layer). This dictates the minimum resolvable size of interpreted features.

An important role of database attribution is to give users information on the provenance (explanation, input data, and references) and confidence in each interpretation. Confidence fields in the databases are qualitative and indicate the repeatability of an interpretation, whether placement (mapping uncertainty) or age (how likely the age assignment is to be changed). We follow the schemes of Markwick (2019; Markwick and Lupia, 2002), which are based on those of Ziegler et al. (1985) and reflect the source(s) of information, data density, and data grain (e.g. cell size). Confidence is not a synonym for uncertainty, which is the quantitative estimation of error present in the data (viz., age uncertainty being the error assigned to an absolute age derived from an analytic technique; a detailed description of confidence attribution is provided in S.I.).

3 Structural Elements Database

The Structural Elements database comprises the following key structural components: faults (features with 'evidence' of displacement), lineaments (features that may be structural but

with no unequivocal offset or other evidence of motion), bedding (S0), folds, and foliation. All have been captured as lines (polylines in ArcGIS) rather than polygons and therefore represent the position of the fault without implying displacement or rock volume loss/repetition.

Although automated methods have been used to identify lineaments using remote sensing datasets (Cascone et al., 2016; Royer et al., 1989), in this study, the majority of features have been captured manually. This reflects problems we have found with automated methods when interpretations are based on multiple, diverse datasets; for example, using breaks in magnetic anomaly data to pick out fracture zones, which may coincide with continuous bathymetric scarps or troughs, and continuous gravity lows (see SI).

The resolution, precision, and accuracy of mapped structural features vary according to the input datasets used in each interpretation resulting in systematic differences between features mapped offshore and onshore (e.g. Angoche or Majunga Basins in comparison to the East African rift system, Figure 3). This combination of resolutions is less problematic than may be expected because it also reflects application as well as data provenance. Structural features in deep-water settings, such as fracture zones, are most frequently used to constrain plate kinematic models, where the detailed mapping within a fracture zone is unnecessary. On continental margins and onshore the availability of often commercially acquired data, including seismic or high-resolution aeromagnetic data and FTG (Full Tensor Gravity Gradiometry) surveys, results in significant variations in mapping resolution. End-users must be aware of the resolution of the database they are using.

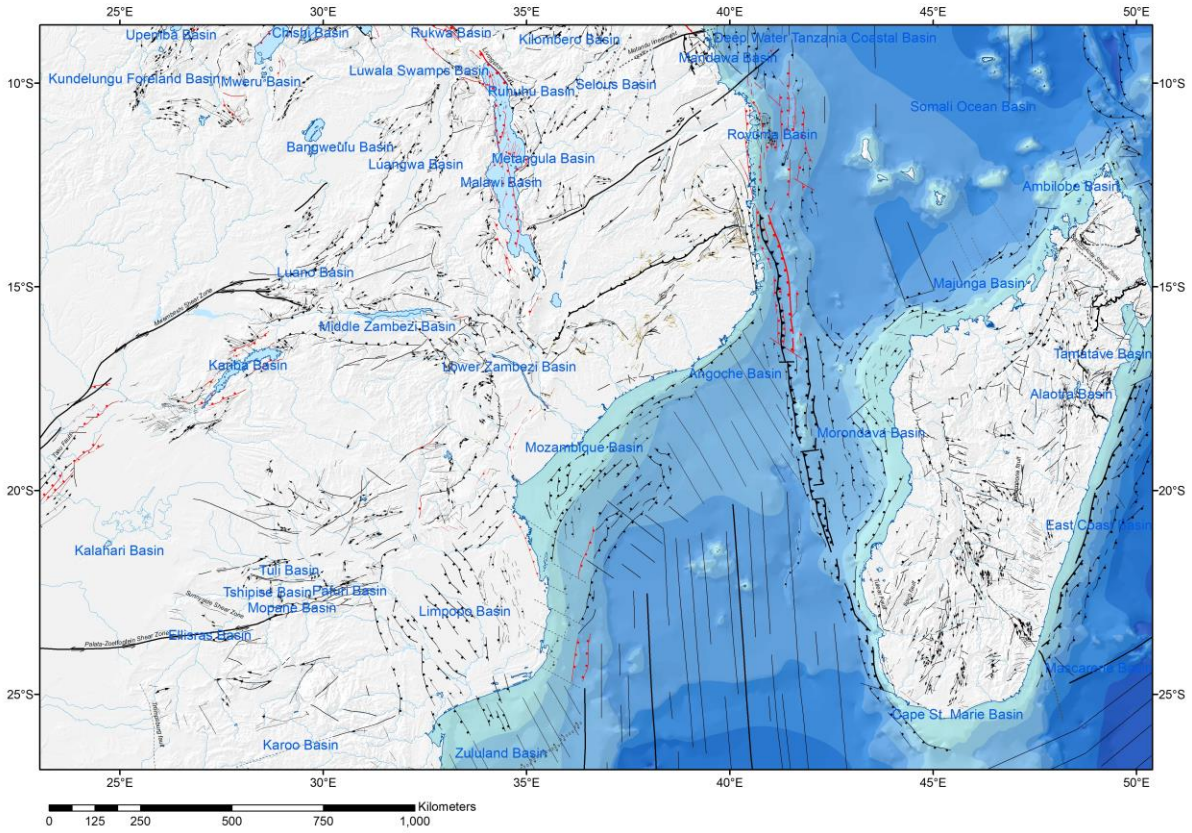

Figure 3. The structural elements database for the southern area of the East Africa margin from Tanzania to the South African border with Mozambique. This exhibits a complex history and variety of tectonic settings to test out the mapping methodologies and workflows. The symbology follows standard conventions for showing kinematics based on that published by the USGS. A full explanation is given in Markwick (2019).

In the deep oceans (e.g. Somali Ocean Basin, Figure 3) where the crust is considered to be relatively homogenous and thin (c.7 km), deviations in the gravity field largely reflect bathymetric changes due to juxtaposed differences in crustal thickness due to faulting, especially spreading ridges, subduction zone transform faults and fracture zones, and igneous extrusions (seamounts and plateaus). These are further exacerbated by compensation effects when using the free-air solution (viz., subduction zones represented by deep gravity lows with the subduction

zone feature drawn along the axis of the lows, corresponding, usually to the deepest part of the corresponding bathymetric trench; spreading ridges represented by narrow gravity lows bounded by highs orientated perpendicular to fracture zones).

Continental margins are typically structurally more complex with a higher density of structuralization than in the deep ocean (e.g. Majunga and Angoche Basins, Figure 3). The workflow used here to capture features is similar, with the main inputs being gravity data and bathymetry. Also, on many margins, the availability of controlled source reflection seismic data, often acquired by industry, provides significantly higher resolution.

The onshore structural mapping is based on more detailed remote sensing data, including radar (SRTM3: 90m resolution), Landsat (30m resolution), and published aeromagnetic data. Also, there is a much higher density of publications, sections, field-based studies, and geological mapping (e.g., Lake Malawi portion of the East African Rift system). Folds are the clearest expression of deformation that can be identified onshore usually using the geometry of topographic ridges. Faults, as lineation's picked out by continuous scarps or narrow valleys that cut the surface fabric, with the highest confidence where these features truncate and offset folds. These are captured using both Landsat and SRTM3 grids.

Landsat is clearest in semi-arid to arid areas where bedrock is exposed, and there is limited vegetation to obscure patterns. In vegetated areas, we have used different bandwidths to pick out subtle changes that may indicate structure. The radar data (SRTM3) can penetrate vegetation but does require topographic relief to be able to identify structures. Derivatives are used to expose geological features, including calculations of slope comparable to the total horizontal derivate used in potential field analysis and high pass filters (see S.I. for details). We have also used different azimuths and sun angles to generate hill-shades to highlight possible topographic features that may indicate structure. Detailed, published aeromagnetic data re used where available. Georeferenced geology maps provide further confirmation of interpretations and are throughout this study to add information on kinematics and timing, where this is not clear from primary data.

The Structural Elements database is used to define sedimentary basins, the nature and geometry of crustal blocks, provide an indication of the dominant stress-field at the time the features were active (geodynamics), and as a guide to landscape response (viz., the position of

scarps through time and river pathways in paleogeography and source-to-sink analysis). Major faults on now separate continental plates can be used to tie pre-rift plate geometries.

4 Igneous Features Database

The Igneous Features database includes information on the geometry, age, petrology, and tectonic environment of intrusive and extrusive (Figure 4). It comprises two feature classes in ArcGIS™, one each for polygons and lines. Most igneous features are mapped as polygons, but igneous dikes are stored mainly as lines - exceptions include large-scale vertical intrusions such Great Dyke of Zimbabwe, which can be up to 11 km wide (Schoenberg et al., 2003). The igneous features database does not maintain topological rules in that features can overlap in certain circumstances.

In the oceans, gravity, bathymetric and magnetic data are used to identify probable igneous features constrained by published papers, dredge samples, and wells. Examples of this include the magma addition to the Somali basin oceanic floor and localized volcanism within the Davie Deformational Zone (Figure 4).

Onshore features are largely constrained using Landsat imagery. Features can be differentiated from surrounding bedrock by color and textural differences (see S.I.), especially in areas of no or limited vegetation and where the volcanics are relatively young (e.g. Rukwa Volcanics, East African Rift, Figure 4). In dense vegetation areas, the morphology of volcanics may be more apparent using radar data and drainage networks; the lower confidence is reflected in the confidence codes. Geological maps and publications are used to assign crystallization ages, petrological, and tectonic setting information.

The Igneous Features database is designed to provide input for constraining plate kinematic reconstructions, geodynamic modeling, and basin modeling (heat-flow). Igneous features are also important in provenance studies, source-to-sink analysis, and paleogeography. This is by influencing the landscape through differential weathering and erosion, vegetation cover, and drainage evolution (drainage can be modified instantaneously by extrusions).

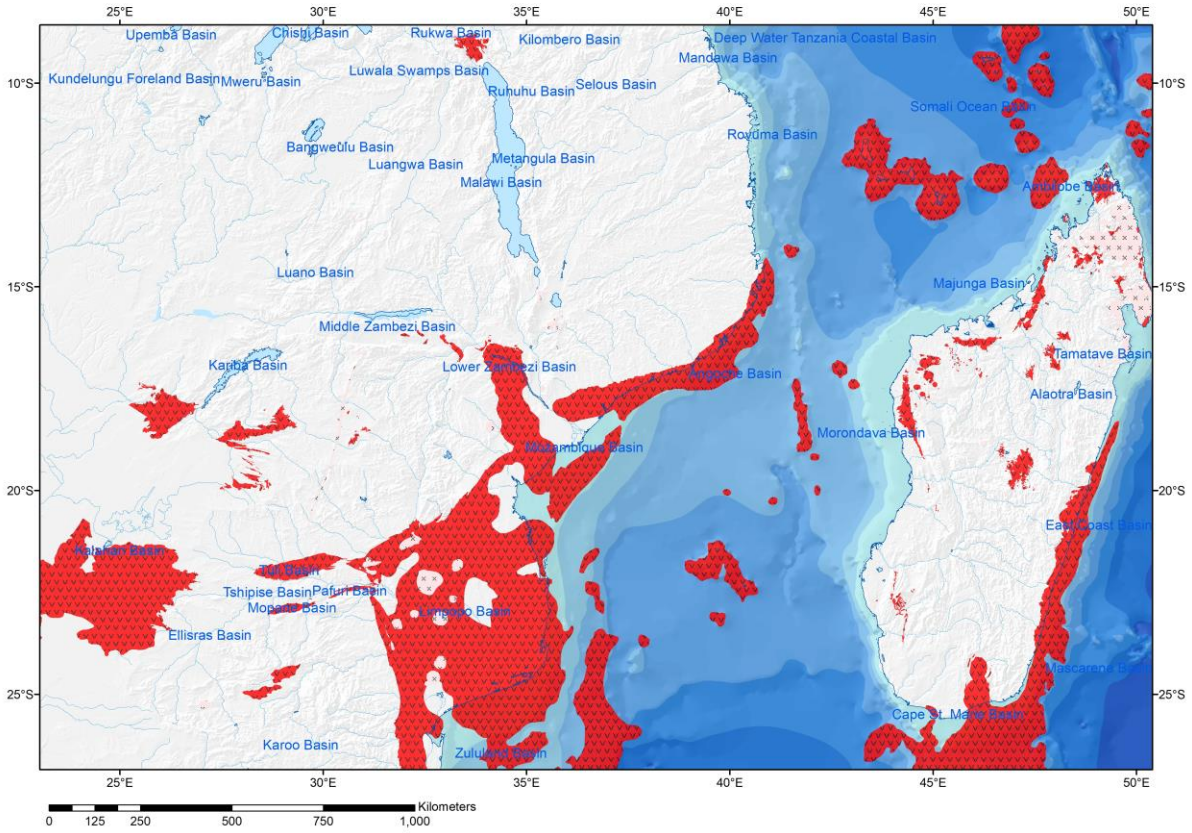

Figure 4. The extent of igneous features mapped for the example study area used in this paper. Red, extrusives; pink, intrusives.

5 Crustal Facies Database

The Crustal Facies database records the geometry, thickness, and composition of the Earth's crust. The crust represents the chemically distinct upper layers of the Earth. Rheologically, the crust forms part of the lithosphere, which must be considered in geodynamic modeling. Where the crust is absent, e.g. in areas of hyper-extension, we incorporate the presence of exhumed mantle.

Existing methods for categorizing crustal types are commonly associated with the processes involved, such as compressional margin, hyper-extended (Péron-Pinvidic and Manatschal, 2010), or volcanic passive margins. This is problematic from a global database

perspective as it combines observations with process while also mixing crustal type with geodynamics.

Here we take a different approach and differentiate by composition (‘continental’, ‘oceanic’, or ‘mantle’) and thickness with reference to 'standard' continental crust of 30-35 km and oceanic crust of 5-7 km (thick, normal, thin, very thin) (Figure 5). The composition reflects the history of that crust (previous tectonic cycles) but is independent of the geodynamic processes acting on the crust once formed. Consequently, interpretations of crustal facies will change through geological time. The default in our databases is the present-day status. Separate databases are built for each timeslice reconstructed as part of the paleogeography workflow (Markwick, 2019).

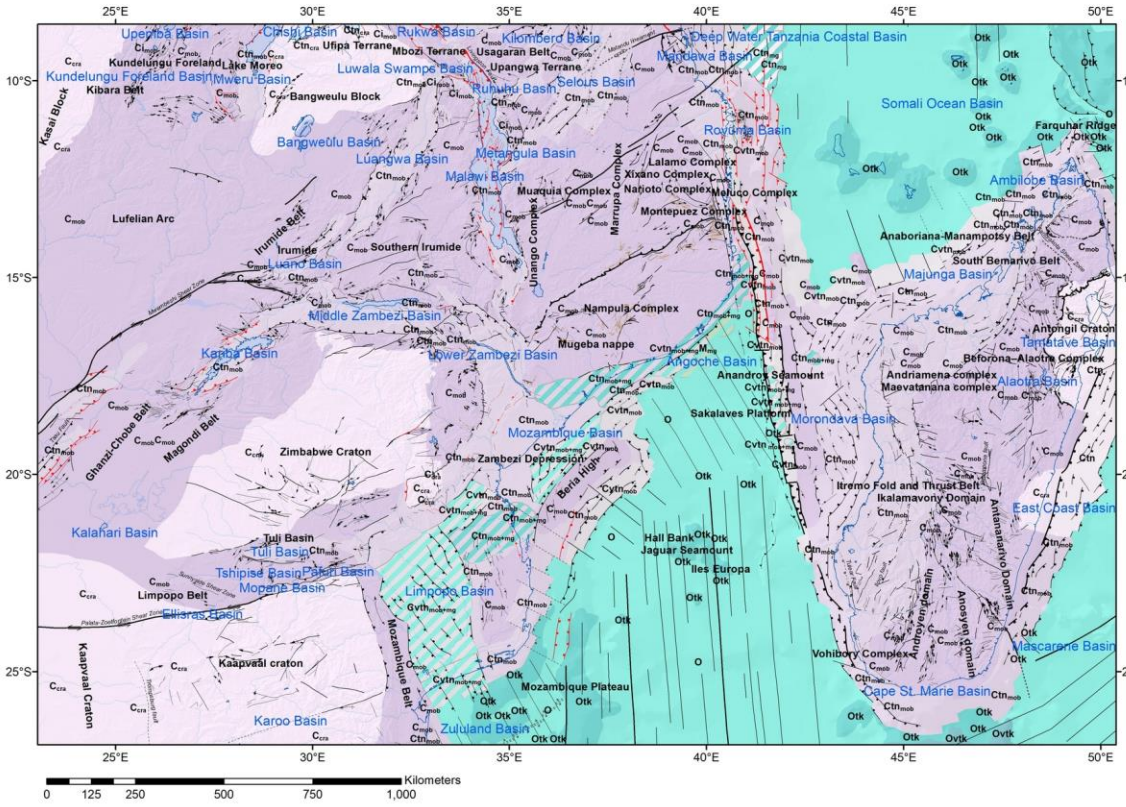
25°E
30°E
35°E
40°E
45°E
50°E
10°S
15°S
20°S
25°S
Upemba Basin
Cisshi Basin
Rukwa Basin
Kilombero Basin
Deep Water Tanzania Coastal Basin
Kundelungu Foreland Basin
Lake Moreo
Mbozi Terrane
Usagaran Belt
Mandawa Basin
Luwala Swamps Basin
Upangwa Terrane
Mweru Basin
Kibara Belt
Bangweulu Block
Ruhuhu Basin
Selous Basin
Somali Ocean Basin
Kasai Block
Bangweulu Basin
Rovuma Basin
Farquhar Ridge
Lúangwa Basin
Metangula Basin
Lalamo Complex
Malawi Basin
Xixano Complex
Natioto Complex
Muaquia Complex
Meluco Complex
Ambilobe Basin
Lufelian Arc
Irumide Belt
Marrupa Complex
Montepuez Complex
Anaboriana-Manampotsy Belt
Irumide
Southern Irumide
Unango Complex
South Bemarivo Belt
Luano Basin
Majunga Basin
Middle Zambezi Basin
Nampula Complex
Antongil Craton
Tamatave Basin
Kariba Basin
Mugeba nappe
Lower Zambezi Basin
Angoche Basin
Beforona–Alaotra Complex
Anandrov Seamount
Andriamena complex
Maevatanana complex
Alaotra Basin
Ghanzi-Chobe Belt
Magondi Belt
Sakalaves Platform
Morondava Basin
Mozambique Basin
Zimbabwe Craton
Zambezi Depression
Beira High
Itremo Fold and Thrust Belt
Ikalamavony Domain
East Coast Basin
Kalahari Basin
Hall Bank
Jaguar Seamount
Iles Europa
Tuli Basin
Tshipise Basin
Pafuri Basin
Mopane Basin
Limpopo Belt
Limpopo Basin
Ellisras Basin
Antananarivo Domain
Androyen Domain
Anosyen Domain
Vohibory Complex
Mascarene Basin
Kaapvaal craton
Mozambique Belt
Mozambique Plateau
Cape St. Marie Basin
Kaapvaal Craton
Karoo Basin
Zululand Basin
0
125
250
500
750
1,000
Kilometers

Map Legend

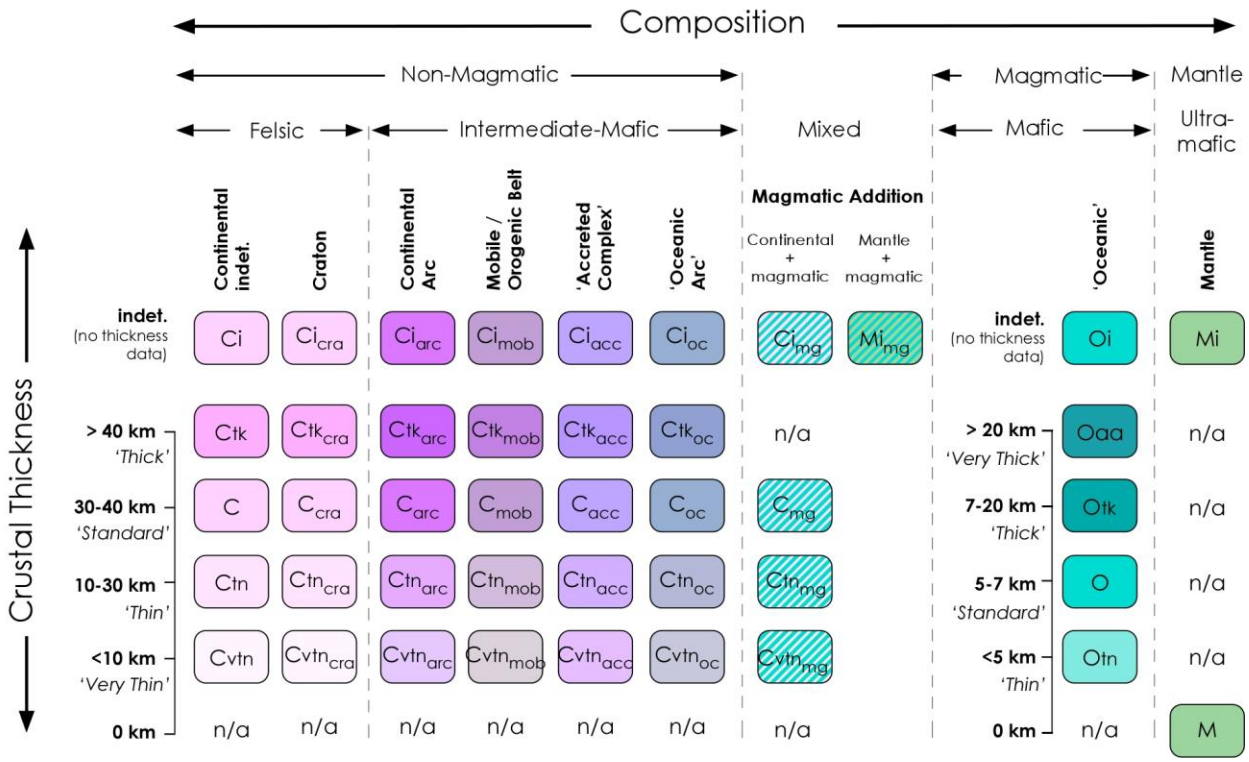
Composition
Non-Magmatic
Magmatic
Mantle
Felsic
Intermediate-Mafic
Mixed
Mafic
Ultra-mafic
Continental indet.
Craton
Continental Arc
Mobile / Orogenic Belt
'Accreted Complex'
'Oceanic Arc'
Magmatic Addition
Continental + magmatic
Mantle + magmatic
'Oceanic'
Mantle
Crustal Thickness
indet. (no thickness data)
> 40 km 'Thick'
30-40 km 'Standard'
10-30 km 'Thin'
<10 km 'Very Thin'
0 km
Ci
Cicra
Ciarc
Cimob
Ciacc
Cioc
Cimg
Mimg
Oi
Mi
Ctk
Ctkcra
Ctkarc
Ctkmob
Ctkacc
Ctkoc
Oaa
C
Ccra
Carc
Cmob
Cacc
Coc
Cmg
Otk
Ctn
Ctncra
Ctnarc
Ctnmob
Ctnacc
Ctnoc
Ctnmg
O
Cvtn
Cvtncra
Cvtnarc
Cvtnmob
Cvtnacc
Cvtnoc
Cvtnmg
Otn
M
n/a

Figure 5. Crustal Facies, including the map legend and abbreviations used.

The different compositions, and corresponding crustal thicknesses, are mapped from an analysis of gravity and magnetic data, geological maps, seismic and 2D profiles. In the oceans thick crust, ocean arcs, and isolated continental blocks, usually have a bathymetric and gravity expression. This expression is readily identified and can be checked against seismic, well, and dredge samples where available. The thick crust on the continents will usually be topographically high if it is in isostatic equilibrium, with a corresponding gravity (Bouguer) signature. Geological data (outcrop samples, well cores, geological maps, and published papers) provide information on the composition, including the igneous features database.

In the offshore, we have followed the work of Williams et al. (2010). They found that amplitude changes in the Bouguer total horizontal derivative (Ba THD) provide information on the transition from 'true' ocean crust to continental crust along many margins - limit of 'standard' ('normal') ocean crust.

The domain between the limit of 'standard' oceanic crust and unstretched continental crust is more problematic. Commonly this is defined as 'transitional crust,' but given the potential variability in margin composition, this forms a significantly ambiguous term that is problematic when applied in the database. Instead of using `transitional crust,` the database uses the following classification, which can be derived directly from available global databases: 1) thin (or very thin) continental crust with no magmatic addition, 2) continental crust with magmatic addition, which incorporates inner seaward dipping reflectors, 3) mantle, 4) mantle with magmatic addition, and 5) thick oceanic crust, which incorporates outer seaward dipping reflections.

The resulting map provides input for defining plate polygons in plate kinematic modeling, reconstructing potential heat flow as a critical input to maturity modeling and geothermal exploration, understanding basin formation and evolution, and paleogeographic reconstruction and paleolandscape dynamics.

6 Geodynamics Database

The Geodynamics database records the age and nature of the last thermo-mechanical event with respect to the palaeogeographic timeslice being reconstructed. The default database records this information for the present-day. This method was first discussed in Markwick and Valdes (2004) as *tectonophysiography*, which described areas above the contemporary base-level and, therefore, areas of net erosion (sediment source areas in source-to-sink analysis). The age of the last thermo-mechanical event was added to better represent the decay of landscapes (Campanile et al., 2007; Pazzaglia, 2003; Tucker and Slingerland, 1994; Van der Beek and Braun, 1998; Whipple and Meade, 2004) following the ideas presented in the 1997 USGS thermo-tectonic age map of the world that was used to model heat-flow following Pollack et al., (1993) and crustal thickness and structure (Mooney et al., 1998).

In this new database, the geodynamic state is assigned to the whole Earth, not just those areas above the contemporary base-level. This is classified into those processes characterized by a dominantly vertical stress field (the response to medium and long-wavelength mantle processes – dynamic topography -, more localized volcanics – hotspots -, flexure and isostatic rebound), and those representing a dominantly horizontal stress field, which is then divided into compressional and extensional settings. The symbology of each thermo-mechanical state is shown as solid color when active at the time of the mapped interval and then by increasing widths of diagonal lines colored with the symbol for anorogenic land as the time since activity increases (Figure 6).

Anorogenic land is the landscape expression of the long-term 'equilibrium' state. This is the 'Monadnock phase' in the geomorphological evolutionary scheme of Strahler (1964), represented by a concave-up hypsometric curve. Geologically, this represents crust in isostatic equilibrium with no tectonic forces acting on it. In reality, the point at which any landscape reaches 'equilibrium' will vary according to the type of thermo-mechanical event, bedrock, vegetation cover, and climate evolution. There is also the added complication of dynamic topography (Burgess and Gurnis, 1995; Lithgow-Bertelloni and Silver, 1998) due to mantle processes that may not have been recognized. In this database, we consider 300 million years as an appropriate global cut-off for the onset of 'anorogenic' conditions. In most settings either

'equilibrium' would have been established long before this, or a subsequent geodynamic 'event' would have occurred and overprinted the original geodynamic effects.

The geodynamics database is used in combination with the crustal facies to assess the response of the landscape and from this to estimate relative paleo-elevation and the geometry of uplifts (viz., mantle driven vertical uplift is typified by broad, long-wavelength uplifts, whilst thin-skinned compressional systems can be more localized). The geodynamic mapping also provides a check on plate modeling since the two will need to show the same implied stress field.

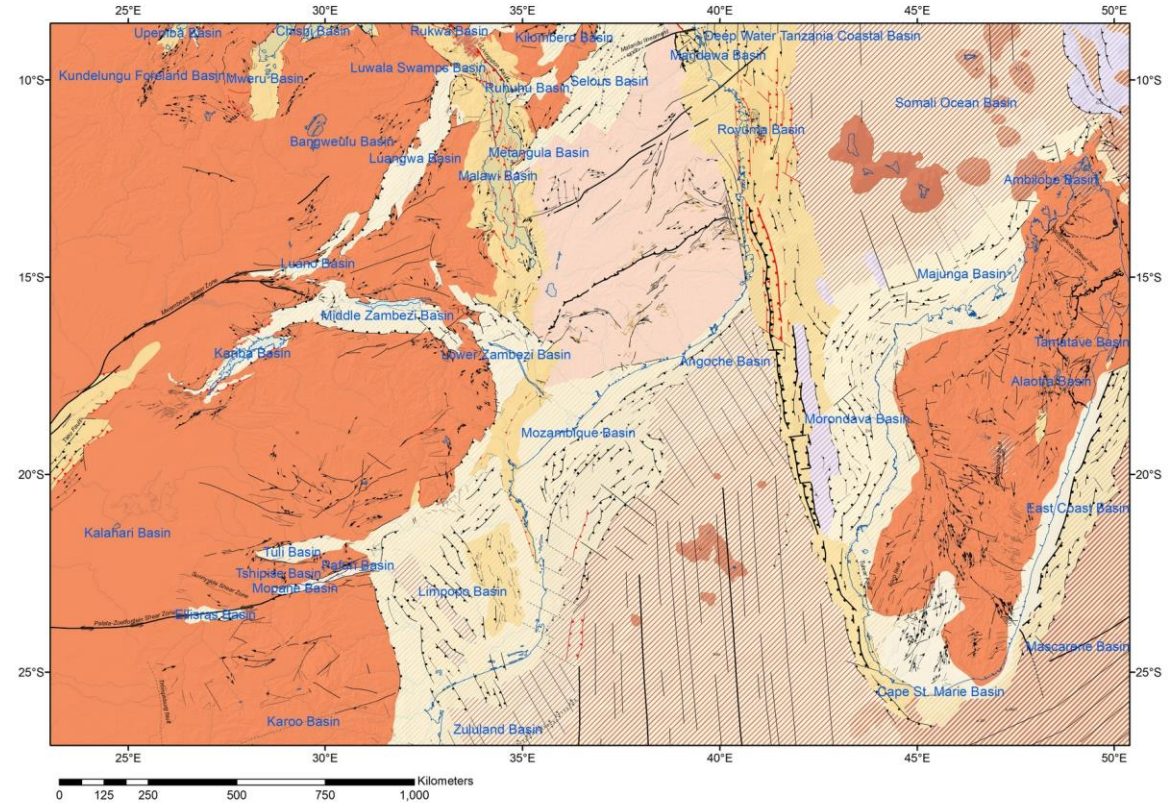

Map Legend

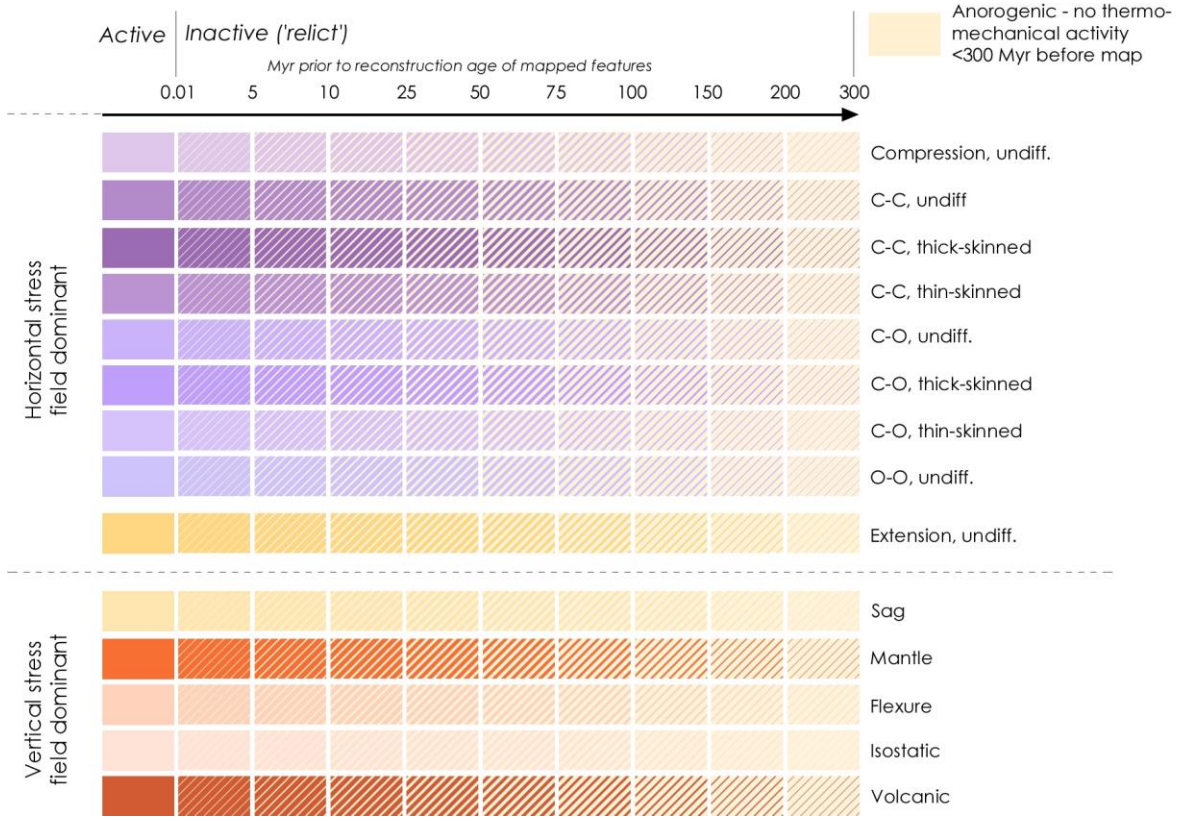

387

Figure 6. The geodynamic state as a representation of the last thermo-mechanical forcing to affect each part of the crust. The legend shows how the time elapsed since activity ceased is incorporated.

7 The East African Crustal Architecture

7.1 The Davie Deformational Zone (DDZ)

Tectonic reconstructions of the East Africa margin are traditionally summarized as a single feature, the "Davie Fracture Zone." This transform boundary was recognized by Scrutton (1978) as a kinematic requirement to accommodate the opening of the West Somali Ocean between Madagascar and Somalia during the Jurassic and Early Cretaceous. Subsequent authors have described a much more complex margin reflecting several tectonic cycles (Jacques et al., 2006; MacGregor et al., 2017; Mahanjane, 2014). Given this complexity, Jacques et al. (2006) recommended the term "Davie Transcurrent Deformation Zone" rather than "Davie Fracture Zone" (DFZ). Our mapping indicates a c.200 km wide deformational zone. But we consider this is a simplification, especially along the Tanzanian and Kenya margins. Deformation is not just strike-slip, so we prefer the term "Davie Deformational Zone" (DDZ).

In this paper, we concentrate on the southern extent of the DDZ (Figures 3 and 5), but have completed mapping of the whole of Sub-Saharan Africa.

The DDZ is partitioned today by major Precambrian and Pan-African structural features. In Mozambique these are the Mwembeshi Shear Zone (MSZ) and Lurio Belt (LB), which act as 'passive' transfer zones. ‘Passive’ because there is no evidence of motion on either fault system during the Mesozoic - Cenozoic formation of the margin, as indicated by Jurassic dyke swarms that cut across the MSZ in Botswana without offset (Igneous Features databases). North of the MSZ, the DDZ includes an outer zone which we postulate to comprise "mixed magmatic thin continental" crust, based on gravity analysis and some limited seismic. This zone of interpreted igneous activity is in line with the last ocean ridge segment and may relate to the spreading ridge's motion along the active transform margin in the Jurassic to Early Cretaceous, and/or the

attempted propagation of spreading into the margin. Igneous activity on the margin is otherwise rare north of the MSZ.

South of the MSZ, the DDZ comprises north-south rifts and ridges, including the Kerimbas and Lacerda grabens. South of the LB the DDZ is dominated by the Davie Ridge, although this is itself complex as indicated by seismic (Bassias, 2016; Mahanjane, 2014) and our mapping. This includes alkaline volcanics which are compositionally similar to the Late Cretaceous volcanics on Madagascar (Bassias and Bertagne, 2015).

Variations in the DDZ coincide with the intersection of Karoo rifts with the margin, for example in the area of the Selous, Rovuma and Rufuji 'Karoo' basins. This part of Gondwana was dissected by Permo-Triassic ('Karoo') rifts (Catuneanu et al., 2005; Delvaux, 2001). Karoo rifting appears to be constrained by the distribution of Precambrian mobile (orogenic) belts (Figure 5).

It is within this complex crustal architecture that Mesozoic breakup occurs with an initial phase of orthogonal rifting along the margin (c.183 – c.170 or 165 Ma, Tuck-Martin et al., 2018), partly dictated by the location of Karoo rifts. This coincided with major volcanism in southern Africa (Igneous Features Database). This was followed by a change in the stress-field c.170 or 165 to c.133 Ma with ocean spreading separating West and East Gondwana (Tuck-Martin et al., 2018). It is during this time that the margin became a transform margin sensu stricto, with a Davie transform fault connecting the coeval spreading ridges of the Somali and Mozambique basins. Whether this was represented by a single fault is questionable, based on the complexities we see on the San Andreas system, Equatorial South America, Agulhas or the northern Caribbean.

When spreading ceased at c.133 Ma (Valanginian), the trace of the transform became obfuscated by subsequent tectonic cycles. This may explain why Klimke and Franke (2016) found no evidence of the transform fault in their seismic study offshore northern Mozambique and Tanzania. However, we suggest that this is also a reflection of the greater reactivation of the DDZ to the south of the MSZ. In the Valanginian, the southern South Atlantic began to open with rifting between the Maurice Ewing Bank and the Tugela crustal promontory, preceded by or coincident with the formation of the volcanic Mozambique Plateau at c.140 Ma.

A further phase of volcanism occurred during the middle Cretaceous and is concentrated mainly on and around Madgascar (c.95-80Ma; Cucciniello et al., 2013; Storey et al., 1997). This has been interpreted as marking the trace of the Marion hotspot (Storey et al., 1997), but is also approximately coincident in time with local plate reorganization, resulting in compression along the DDZ (Figure 6). Intawong et al. (2019) have interpreted this as possible incipient subduction of Middle Jurassic Angoche Basin ocean crust beneath the Davie Ridge. Our mapping based on published seismic and potential fields data shows that the MSZ bounds the northern extent of this compression (Figure 6). Whether this is subduction sensu stricto is questionable – there is no evidence of arc development. But the orientation of fracture zones in the oceanic Angoche Basin and their truncation along this feature (Figure 5) would suggest some loss of surface area due to overthrusting of Madagascar along this boundary.

Superimposed on this history are Cenozoic rifting (East African Rift System, EARS) and mantle dynamics (Dynamic topography) (Figure 6). Today, seismicity along the DDZ is mostly limited to the Cenozoic rifts offshore Kenya, and the line of the DDZ from the MSZ south to the southern Morondava Basin (USGS, 2019). Earthquakes in this region have extensional, not strike-slip focal solutions (Grimison and Chen, 1988) and are related to active rifting across the region. This is clearly shown in the databases by differentiating structures based on whether there is evidence of recent activity (red symbology) or not (black symbology) (Figure 3).

7.2 The Interplay of Pre-existing Fabrics.

The role of inheritance on tectonics has been documented since the 19th century (Şengör et al., 2018). Phillips et al., (2016) found that large-scale shear zones on the Norwegian margin act as a “template” for fault initiation. This may explain our observations in East Africa. We have seen (Figures 3, 5) how crustal-scale Precambrian boundaries (Mwembeshi SZ and Lurio Belt) dictate the partitioning of the DDZ.

The distribution of Karoo basins is similarly dictated by the distribution of Precambrian and Pan-African mobile (orogenic belts) (Figure 5). Karoo basins on the Kaapvaal craton are dominantly foreland basins or sags. The longevity of these Karoo basins and their accommodation space varies depending on orientation and location. For example, the N-S

474 Rukwa and E-W Middle Zambezi basins have relatively long depositional histories (Catuneanu
475 et al., 2005; Roberts et al., 2004). But the NW-SE orientated Luangwa Basin stratigraphy has a
476 major hiatus after the Triassic (Catuneanu et al., 2005) but a geomorphic and depositional
477 activity today. These basins influence the distribution of present-day rivers, but also the locus of
478 Cenozoic rifting and volcanism, for example, the Rungwe volcanics Figure 7).

479

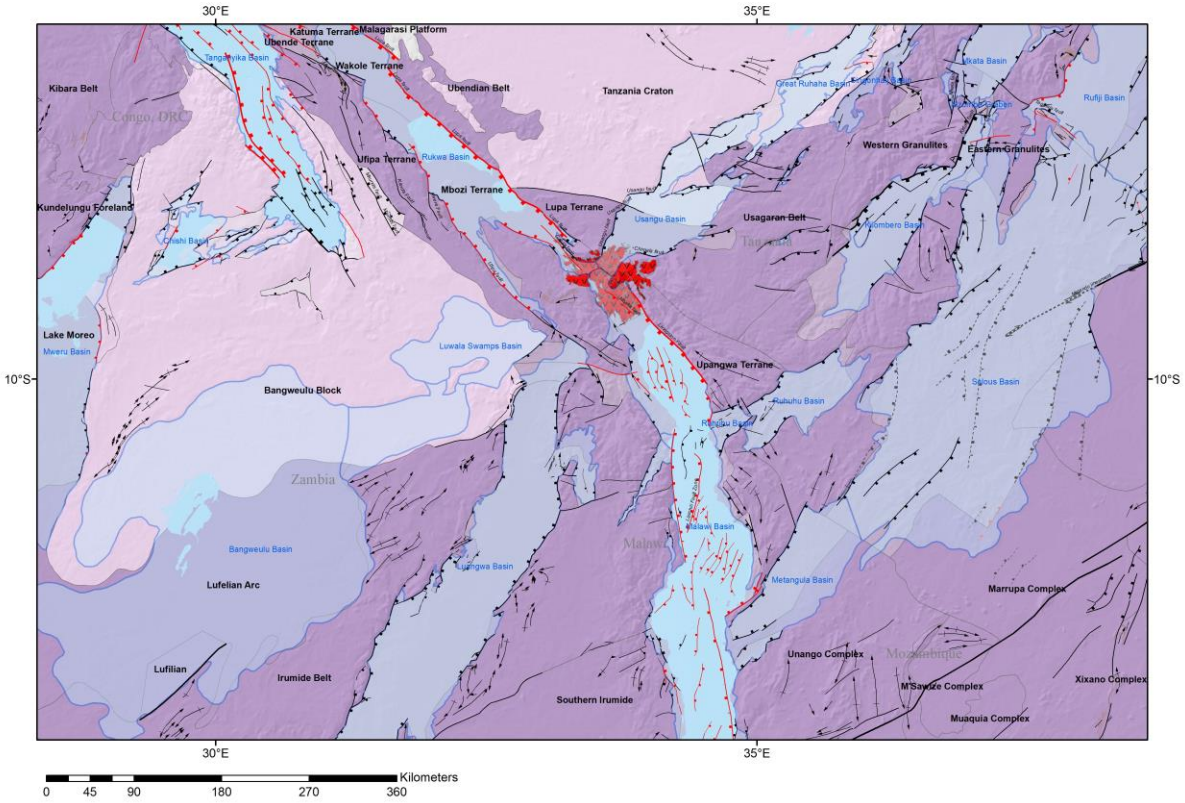

480

481 **Figure 7**. An example of the full database resolution for the Eastern Branch of the East African
482 Rift system illustrating the Structural Elements and Igneous Features databases.

483

484 But the Cenozoic picture is far from simple. The Cenozoic northern Malawi Basin
485 reactivates the older Karoo Rukwa Basin, influenced by the pre-existing Pan-African fabric
486 (Mortimer et al., 2016; Mortimer et al., 2007). But to the south, the N-S Cenozoic Malawi rift
487 cuts across the NW-SE orientated Karoo Metangula and Ruhuhu basins, although these do alter
488 the rift Malawi geometry (Figure 5). The Malawi Rift is orthogonal to the strike of the

Mwembeshi Shear zone with only minor effect. This complicated relationship between pre-existing fabrics and rifting is seen even more clearly in Tanzania in which rifting propagates into cratonic crust - the Northern Tanzania Divergence (Ebinger et al., 1997; Foster et al., 1997; Smith and Mosley, 1993; Yang and Chen, 2010) (Figure 8). A similar evolution has been described by Paton et al. (2017) in the South Atlantic, with initial rifting following the pre-existing crustal fabric (Cape Fold Belt) but then, with a change in the dominant stress-field, a second phase of rifting cut across all fabrics. By interrogating the baseline databases we can see the interplay of structure, crustal facies, geodynamics, and igneous activity—for example, the location of the Rungwe volcanics at the intersection of Karoo and Cenozoic rifts. But the databases also provide the opportunity to quantify this.

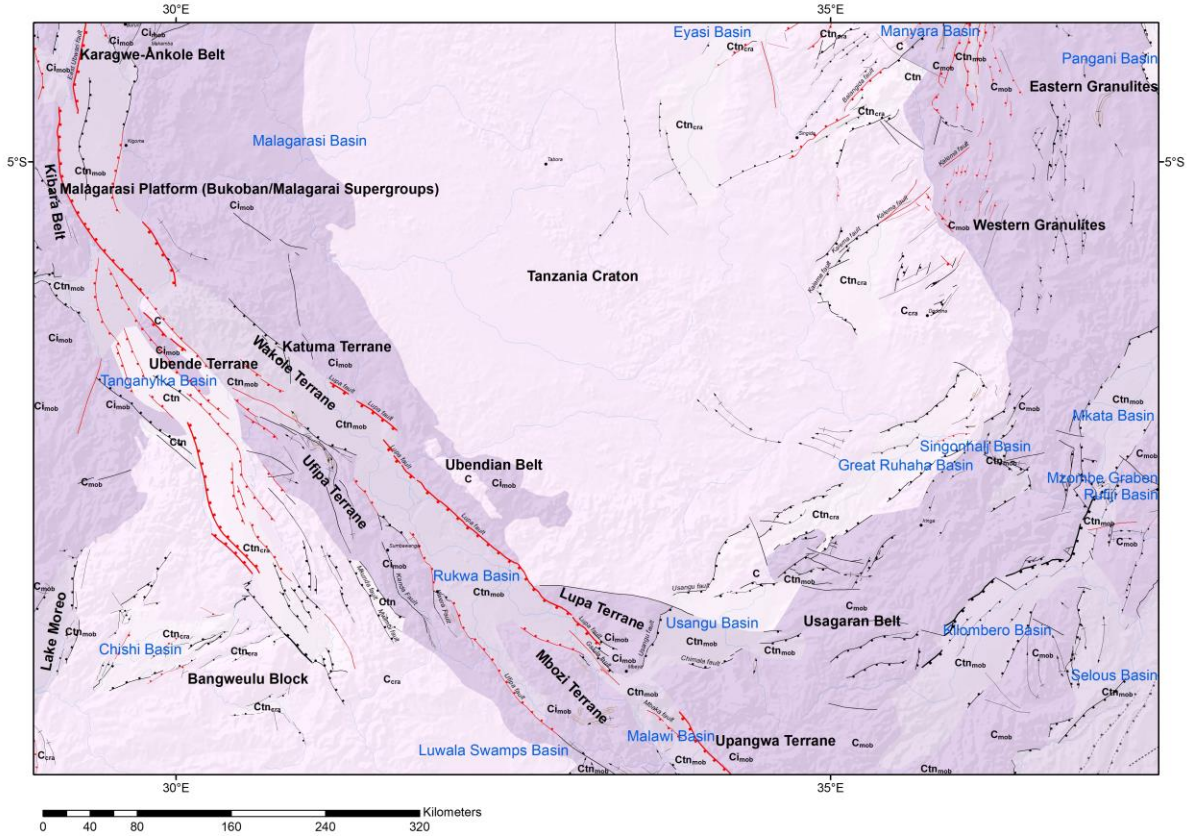

Figure 8. A detail showing the propagation of Late Cenozoic rifting into cratonic crust of the Tanzania craton and Bangwueulu Block.

7.3 The Beira High and Mozambique Lowlands.

The nature of the crust underlying the Beira High and Mozambique lowlands has been a source of uncertainty for decades because of the sparsity of published data. This is an active petroleum exploration area given the gas discoveries at Pande and Termane on the Mozambique coast and oil and gas in the Rovuma Basin. In the last decade, seismic (Mahanjane, 2012) and 2D potential fields modeling (Mueller, 2017) have been published that clarify the continental origin of the Beira High and its relationship to the hinterland. This is seen in our databases Figure 9, which expand interpretations into the Mozambique lowlands, which is still poorly resolved (Figure 9b shows a map of our mapping confidence for the crustal facies interpretations – this assigned mapping confidence provides the opportunity to assess the viability of alternative hypotheses). The Beira High is interpreted as a rifted continental block, bounded landward by a failed rift with SDRs (Senkans et al., 2019), represented in our crustal facies scheme by mixed magmatic – continental crust. The margin narrows to the east in the Angoche Basin. We postulate that this variation may reflect the interplay with Karoo basins. Gravity lows in the northern Mozambique lowlands are consistent with this failed rift continuing westward. However, in our current interpretation there is a spur of thin, non-magmatic continental crust that seems incongruous and requires further modelling and/or seismic coverage (this is a key aim of the baseline databases to identify equivocal interpretations and data gaps that require further investigation).

The crustal interpretation over much of the rest of the Mozambique lowlands is more problematic. Well data show that volcanics floor much of the region, likely related to the Lebombo Karoo volcanics (c.182-180 Ma; Duncan et al., 1997; Riley et al., 2004). But whether these volcanics erupted onto early formed ocean crust or thin continental crust is less clear. Our interpretation of the existing potential fields, seismic and well data shows a band of continental crust along the margin, with thin mixed magmatic -continental crust behind, similar to what is mapped for the Biera High area. The use of the mixed magmatic classification requires that volcanics and thinning were coeval and related. A complication here are circular features in the

high-resolution aeromagnetic data that have been interpreted as calderas (Ruotoistenmäki, 2008) but which have a similar concentric form to intrusions.

Rifting parallel to the Lebombo margin is reported in various commercial studies and is shown in Davison and Steel (2017). The satellite gravity data and magnetics support this.

Our mapping suggests a two-phase opening of the Mozambique basin based on the change in orientation of interpreted fracture zones, which is constrained by recently published magnetic data (Mueller, 2017). This two-phase opening is consistent with the change in the coeval opening of the West Somali basin (Phethean et al., 2016; Tuck-Martin et al., 2018).

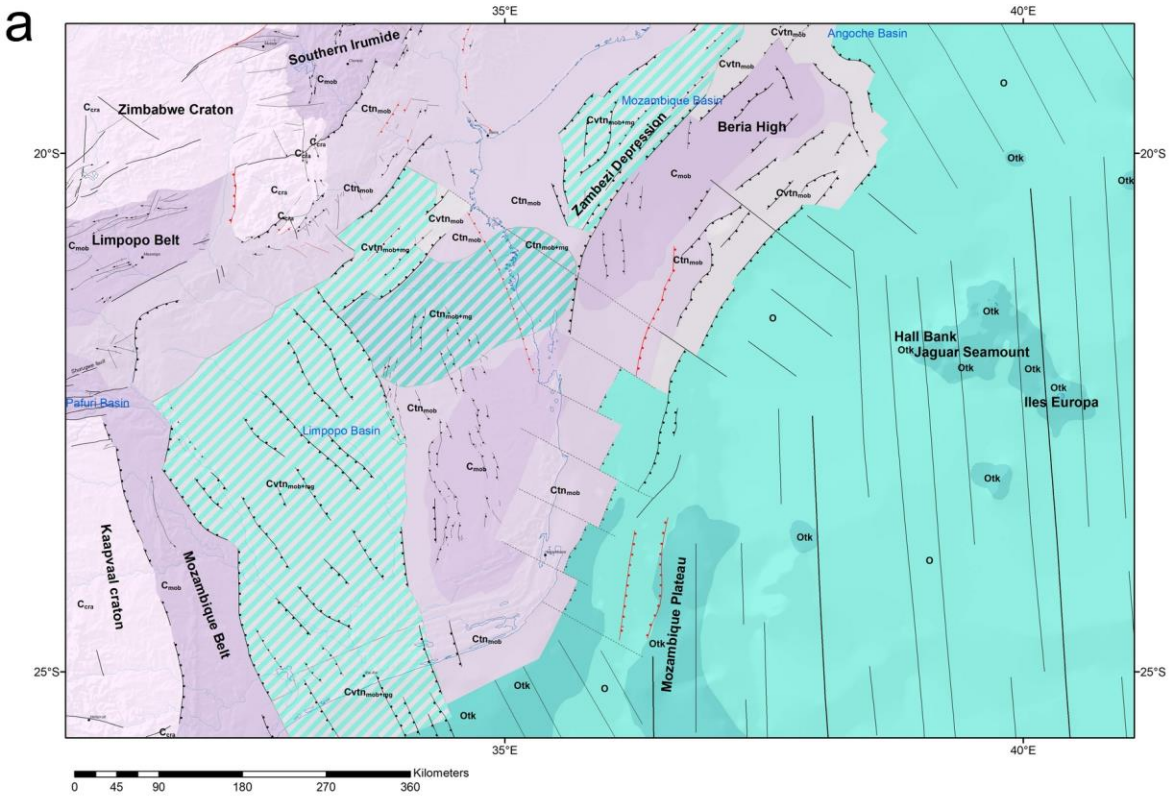
a
35°E
40°E
20°S
25°S
Southern Irumide
Zimbabwe Craton
Limpopo Belt
Angoche Basin
Mozambique Basin
Zambezi Depression
Beria High
Hall Bank
Jaguar Seamount
Iles Europa
Pafuri Basin
Limpopo Basin
Kaapvaal craton
Mozambique Belt
Mozambique Plateau
Otk
0 45 90 180 270 360 Kilometers

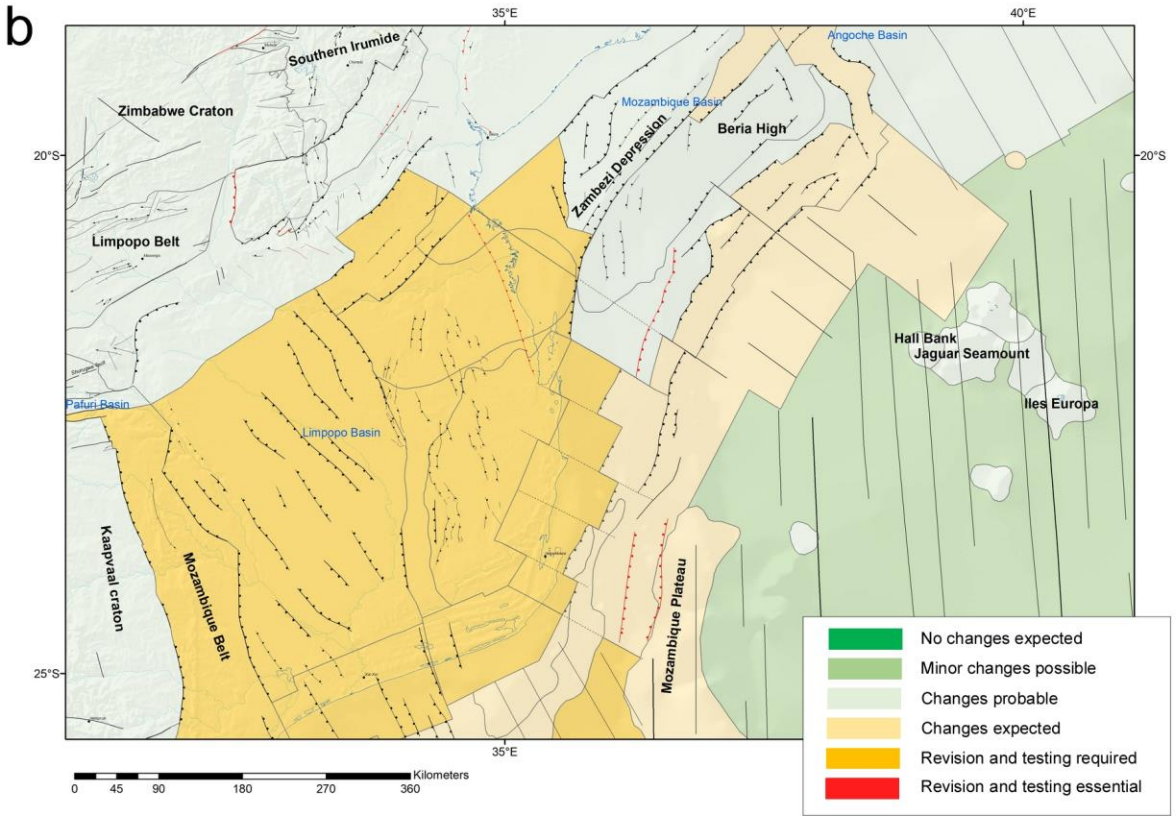
b
35°E
40°E
20°S
25°S
Southern Irumide
Zimbabwe Craton
Limpopo Belt
Angoche Basin
Mozambique Basin
Zambezi Depression
Beria High
Hall Bank
Jaguar Seamount
Iles Europa
Pafuri Basin
Limpopo Basin
Kaapvaal craton
Mozambique Belt
Mozambique Plateau
0 45 90 180 270 360 Kilometers
No changes expected
Minor changes possible
Changes probable
Changes expected
Revision and testing required
Revision and testing essential

539

Figure 9. A detail showing **(a)** the relationship of the nature and geometry of our proposed crustal facies for the Biera High and Mozambique lowlands, see figure 5 for explanation of symbology, **(b)** the mapping confidence assigned to the crustal interpretations. A full explanation of the mapping confidence scheme is provided in the S.I.

8 Final Remarks

Reclus is an open resource designed to provide researchers with a comprehensive, audited, baseline suite of databases upon which to further their own research and our understanding of the tectonics of the Earth system. In this paper, four components have been described: structural elements; igneous features; crustal facies; geodynamics. These features are interpreted from primary data (Landsat, radar, seismic, well data, gravity, and magnetics) supported by secondary data sources (geological maps, literature, pubished academic studies, reports). Elements within each database have been interpreted using a systematic, integrated workflow. Applications of the databases range from tectonics and basin dynamics to mineral and hydrocarbon exploration, hydrogeology, and paleogeography. We envisage that the *Reclus* databases will continue developing and improving as more research is added to them.

The examples shown in this paper illustrate how a systematic approach to capturing tectonic information can provide insights on the juxtaposition and geometry of crustal and structural features in a complex geological area such as East Africa and pose new hypotheses to explain them. The superimposition of and interplay between successive tectonic cycles is much clearer when viewed regionally and systematically.

Only by considering detailed phenomena within the context of the big picture can we fully understand how the system works.

Acknowledgments, Samples, and Data

The ArcGIS databases described in this paper will be made available as part of the supporting information for this Technical Report. This includes the background documentation for each database. The databases will also be available for download through the following website after publication www.knowing.earth

References

Bally, A. W., D. G. Roberts, D. Sawyer, and A. Sinkewich (2012), Tectonic and basin maps of the world, in *Regional geology and tectonics: Phanerozoic passive margins, cratonic basins and global tectonic maps*, edited by D. G. Roberts and A. W. Bally, pp. 970-1025, 1027-1106, 1108-1151, Elsevier. https://doi.org/10.1016/B978-0-444-56357-6.00024-X

Bassias, Y. (2016), Was the Mozambique channel once scattered with islands?, *GEOExPro*, *13*(5), http://www.geoexpro.com/articles/2016/12/was-the-mozambique-channel-once-scattered-with-islands

Bassias, Y., and R. Bertagne (2015), Uplift and erosion of the Davie Fracture Zone, in *PESGB/ HGS Conference on African E&P*, edited, PESGB, London, https://www.researchgate.net/publication/283844849_Uplift_and_Erosion_of_the_Davie_Fracture_Zone

Bird, P. (2003), An updated digital model of plate boundaries, *Geochemistry, Geophysics, Geosystems*, *4*(3). https://doi.org/10.1029/2001GC000252

Brownfield, M. E. (2016), Geologic assessment of undiscovered hydrocarbon resources of Sub-Saharan Africa, in *United States Geological Survey Bulletin*, edited, p. 13. https://doi.org/10.3133/ds69GG

Burgess, P. M., and M. Gurnis (1995), Mechanisms for the formation of cratonic stratigraphic sequences, *Earth and Planetary Science Letters*, *136*, 647-663. https://doi.org/10.1016/0012-821X(95)00204-P

Campanile, D., C. G. Nambiar, P. Bishop, M. Widdowson, and R. Brown (2007), Sedimentation record in the Konkan-Kerala Basin: implications for the evolution of the Western Ghats and the Western Indian passive margin, *Basin Research*, *20*(1), 3-22. https://doi.org/10.1111/j.1365-2117.2007.00341.x

Cascone, L., C. Green, S. Campbell, A. Salem, and D. Fairhead (2016), ACLAS - a method to define geologically significant lineaments from potential-field data, *Geophysics*, *82*(4), G87-G100. https://doi.org/10.1190/geo2016-0337.1

Catuneanu, O., H. Wopfner, P. G. Eriksson, B. Cairncross, B. S. Rubidge, R. M. H. Smith, and P. J. Hancox (2005), The Karoo basins of south-central Africa, *Journal of African Earth Science*, *43*(1-3), 211-253. https://doi.org/10.1016/j.jafrearsci.2005.07.007

CGG Robertson (2020), Sedimentary basins of the world, edited, ESRI, ESRI Living Atlas, http://www.arcgis.com/home/item.html?id=a15e179c3b6a45ef94107353c2f64fc1

CGMW (2010), Tectonic map of Africa, Commission for the Geological Map of the World.

Chamot-Rooke, N., C. Rangin, X. Le Pichon, and DOTMED Working Group (2005), *DOTMED : A synthesis of deep marine data in eastern Mediterranean*, 64 pp., Société géologique de France, Paris.

Coffin, M. F., and O. Eldholm (1994), Large igneous provinces: Crustal structure, dimensions, and external consequences, *Reviews of Geophysics*, *32*(1), 1-36. https://doi.org/10.1029/93RG02508

Cucciniello, C., L. Melluso, F. Jourdan, J. J. Mahoney, T. Meisel, and V. Morra (2013), ^{40}Ar–^{39}Ar ages and isotope geochemistry of Cretaceous basalts in northern Madagascar: refining eruption ages, extent of crustal contamination and parental magmas in a flood basalt province, *Geological Magazine*, *150*(1), 1-17. https://doi.org/10.1017/S0016756812000088

Davison, I., and I. Steel (2017), Geology and hydrocarbon potential of the East African continental margin: a review, *Petroleum Geoscience*, *24*, 57-91. https://doi.org/10.1144/petgeo2017-028

Delvaux, D. (2001), Karoo rifting in western Tanzania: precursor of Gondwana break-up?, in *Contributions to Geology and Paleontology of Gondwana. In honour of Prof. Dr. Helmut Wopfner*, edited, pp. 111-125, Royal Museum for Central Africa, Universität zu Köln, http://www.africamuseum.be/research/publications/elsewhere/pub_view?pubid=883

Delvaux, D., M. Kraml, M. Sierralta, A. Wittenberg, J. W. Mayalla, K. Kabaka, C. Makene, and GEOTHERM working group (2010), Surface Exploration of a Viable Geothermal Resource in Mbeya area, SW Tanzania. Part I: Geology of the Ngozi – Songwe Geothermal System, paper presented at World Geothermal Congress 2010, 25-29 April 2010 Bali, Indonesia.

Duncan, R. A., P. R. Hooper, J. Rehacek, J. S. Marsh, and A. R. Duncan (1997), The timing and duration of the Karoo igneous event, southern Gondwana, *Journal of Geophysical Research B. Solid Earth and Planets*, *102*(B8), 18127-18138. https://doi.org/10.1029/97JB00972

Ebinger, C. J., Y. P. Djomani, E. Mbede, A. Foster, and J. B. Dawson (1997), Rifting Archaean lithosphere: the Eyasi-Manyara-Natron rifts, East Africa, *Journal of the Geological Society, London*, *154*(6), 947-960. https://doi.org/10.1144/gsjgs.154.6.0947

ESRI (2017), ArcGIS Desktop, edited, Environmental Systems Research Institute, Redlands, CA, https://gis.stackexchange.com/questions/5783/how-do-you-cite-arcgis

Exxon Production Research Company (1985), Tectonic map of the world, *prepared by the World Mapping Project as part of the Tectonic map series of the world*, American Association of Petroleum Geologists Foundation, Tulsa, OK.

Farr, T. G., et al. (2007), The Shuttle Radar Topography Mission, *Reviews of Geophysics*, *45*, 1-33. https://doi.org/10.1029/2005RG000183

Foster, A., C. J. Ebinger, E. Mbede, and D. C. Rex (1997), Tectonic development of the northern Tanzania sector of the East African Rift System, *Journal of the Geological Society, London*, *154*(4), 689-700. https://doi.org/10.1144/gsjgs.154.4.0689

Gahagan, L. M., et al. (1988), Tectonic fabric map of the ocean basins from satellite altimetry data, *Tectonophysics*, *155*, 1-26. https://doi.org/10.1016/0040-1951(88)90258-2

Global Volcanism Program (2019), Volcanoes of the World, v.4.8.2., E. Venke, Smithsonian Institution. https://doi.org/10.5479/si.GVP.VOTW4-2013

Grimison, N. L., and W.-P. Chen (1988), Earthquakes in the Davie Ridge - Madgascar region and the southern Nubian - Somalian plate boundary, *Journal of Geophysical Research. Solid Earth*, *93*(B9), 10439- 104500. https://doi.org/10.1029/JB093iB09p10439

Heidbach, O., et al. (2018), The World Stress Map database release 2016: Crustal stress pattern across scales, *Tectonophysics*, *744*, 484-498. https://doi.org/10.1016/j.tecto.2018.07.007

Hicks, N., and A. Green (2017), A first assessment of potential stratigraphic traps for geological storage of CO_2 in the Durban Basin, South Africa, *International Journal of Greenhouse Gas Control*, *64*, 73-86. https://doi.org/10.1016/j.ijggc.2017.06.015

Hunt, T. S. (1873), The paleogeography of the North-American continent, *Journal of the American Geographical Society of New York*, *4*, 416-431, http://www.jstor.org/stable/196403

Intawong, A., N. Hodgson, K. Rodriguez, and P. Hargreaves (2019), Oil prospects in the Mozambique Channel: where incipient subduction meets passive margin, *First Break*, *37*, 75-81,

IOC, IHO, and BODC (2003), Centenary Edition of the GEBCO Digital Atlas on behalf of the Intergovernmental Oceanographic Commission and the International Hydrographic Organization as part of the General Bathymetric Chart of the Oceans, British Oceanographic Data Centre, Liverpool, https://www.bodc.ac.uk/projects/data_management/international/gebco/gebco_digital_atlas/

Jacques, J. M., K. L. Wilson, P. J. Markwick, and D. G. Wright (2006), The Importance of the 'Davie Transcurrent Deformation Zone' on hydrocarbon prospectivity of the offshore blocks of the Rovuma and Tanzanian Coastal Basins, East Africa, paper presented at AAPG International Conference and Exhibition, 5-8, November 2006, Perth, West Australia.

Johnston, A. K. (1856), *The physical atlas of natural phenomena*, 137 pp., William Blackwood & Sons, London.

Kim, S.-S., and P. Wessel (2011), New global seamount census from the altimetry-derived gravity data, *Geophysical Journal International*, *186*(2), 615-631. https://doi.org/10.1111/j.1365-246X.2011.05076.x

Klimke, J., and D. Franke (2016), Gondwana breakup: no evidence for a Davie Fracture Zone offshore northern Mozambique, Tanzania and Kenya, *Terra Nova*, *28*, 233-244. https://doi.org/10.1111/ter.12214

Kraml, M., N. Ochmann, D. Leible, T. Kling, S. A. Chiragwile, M. Jodocy, H. Kreuter, and GPT Exploration Team (2014), Results of the Pre-Feasibility Study on Ngozi Geothermal Project in Tanzania, paper presented at The 5th African Rift Geothermal Conference, 27th October to 2nd November 2014, Arusha, Tanzania.

Lesur, V., M. Hamoudi, Y. Choi, J. Dyment, and E. Thébault (2016), Building the second version of the World Digital Magnetic Anomaly Map (WDMAM), *Earth, Planets and Space*, *68*(27). https://doi.org/10.1186/s40623-016-0404-6

Lithgow-Bertelloni, C., and P. G. Silver (1998), Dynamic topography, plate driving forces and the African superswell, *Nature*, *395*, 269-272. https://doi.org/10.1038/26212

Macgregor, D. S. (2015), History of the development of the East African Rift System: A series of interpreted maps through time, *Journal of African Earth Science*, *101*, 232-252. https://doi.org/10.1016/j.jafrearsci.2014.09.016

MacGregor, D. S., J. Argent, and P. Sansom (2017), Introduction to the thematic set: Tectonics and petroleum systems of East Africa, *Petroleum Geoscience*, *24*, 3-7. https://doi.org/10.1144/petgeo2017-105

Mahanjane, E. S. (2012), A geotectonic history of the northern Mozambique Basin including the Beira High – A contribution for the understanding of its development, *Marine and Petroleum Geology*, *36*(1), 1-12. https://doi.org/10.1016/j.marpetgeo.2012.05.007

Mahanjane, E. S. (2014), The Davie Fracture Zone and adjacent basins in the offshore Mozambique Margin – A new insights for the hydrocarbon potential, *Marine and Petroleum Geology*, *57*, 561-571. https://doi.org/10.1016/j.marpetgeo.2014.06.015

Markwick, P. J. (2019), Palaeogeography in exploration, *Geological Magazine (London)*, *156*(2), 366-407. https://doi.org/10.1017/S0016756818000468

Markwick, P. J., and R. Lupia (2002), Palaeontological databases for palaeobiogeography, palaeoecology and biodiversity: a question of scale, in *Palaeobiogeography and biodiversity change: a comparison of the Ordovician and Mesozoic-Cenozoic radiations*, edited by J. A. Crame and A. W. Owen, pp. 169-174, Geological Society, London, London. https://doi.org/10.1144/GSL.SP.2002.194.01.13

Markwick, P. J., and P. J. Valdes (2004), Palaeo-digital elevation models for use as boundary conditions in coupled ocean-atmosphere GCM experiments: a Maastrichtian (late Cretaceous) example, *Palaeogeography, Palaeoclimatology, Palaeoecology*, *213*, 37-63. https://doi.org/10.1016/j.palaeo.2004.06.015

Martinelli, G., G. Dongarrà, M. Q. W. Jones, and A. Rodriguez (1995), Geothermal Features of Mozambique - Country Update, paper presented at World Geothermal Congress, Florence, Italy, 18-31 May.

Maus, S., T. Sazonova, K. Hemant, J. D. Fairhead, and D. Ravat (2007), National Geophysical Data Center candidate for the World Digital Magnetic Anomaly Map, *Geochemistry, Geophysics, Geosystems*, *8*. https://doi.org/10.1029/2007GC001643

Maus, S., et al. (2009), EMAG2: A 2-arc min resolution Earth Magnetic Anomaly Grid compiled from satellite, airborne, and marine magnetic measurements, *Geochemistry, Geophysics, Geosystems*, *10*. https://doi.org/10.1029/2009GC002471

Mnjokava, T. T. (2012), Geothermal exploration in Tanzania - status report, in *Short Course VII on Exploration for Geothermal Resources, organized by UNU-GTP, GDC and KenGen, at Lake Bogoria and Lake Naivasha, Kenya, Oct. 27 – Nov. 18, 2012*, edited, Lake Bogoria and Lake Naivasha, Kenya, https://orkustofnun.is/gogn/unu-gtp-sc/UNU-GTP-SC-15-1003.pdf

Mooney, W. D., G. Laske, and T. G. Masters (1998), CRUST 5.1: A global crustal model at 5° x 5°, *Journal of Geophysical Research B. Solid Earth and Planets*, *103*(B1), 727-747. https://doi.org/10.1029/97JB02122

Mortimer, E. J., D. A. Paton, C. A. Scholz, and M. R. Strecker (2016), Implications of structural inheritance in oblique rift zones for basin compartmentalization: Nkhata Basin, Malawi Rift (EARS), *Marine and Petroleum Geology*, *72*, 110-121. https://doi.org/10.1016/j.marpetgeo.2015.12.018

Mortimer, E. J., D. A. Paton, C. A. Scholz, M. R. Strecker, and P. Blisniuk (2007), Orthogonal to oblique rifting: effect of rift basin orientation in the evolution of the North basin, Malawi Rift, East Africa, *Basin Research*, *19*(3), 393-407. https://doi.org/10.1111/j.1365-2117.2007.00332.x

Mueller, C. O. (2017), The Central Mozambique continental margin - Its tectonic evolution as the centrepiece of the initial Gondwana break-up, 227 pp, University of Bremen, Bremerhaven.

Müller, R. D., M. Sdrolias, C. Gaina, and W. R. Roest (2008), Age, spreading rates, and spreading asymmetry of the world's ocean crust, *Geochemistry, Geophysics, Geosystems*, *9*, Q04006. https://doi.org/10.1029/2007GC001743

Müller, R. D., W. R. Roest, J.-Y. Royer, L. M. Gahagan, and J. G. Sclater (1997), Digital isochrons of the world's ocean floor, *Journal of Geophysical Research*, *102*, 3211-3214. https://doi.org/10.1029/96JB01781

NASA Landsat Program (2000), Landsat, USGS, Sioux Falls, South Dakota, http://glcf.umd.edu/data/landsat/

Paton, D. A., E. J. Mortimer, N. Hodgson, and D. Van der Spuy (2017), The missing piece of the South Atlantic jigsaw: when continental break-up ignores crustal heterogeneity, in *Petroleum Geoscience of the West Africa Margin*, edited by T. Sabato Ceraldi, R. A. Hodgkinson and G. Backe, pp. 195-210, Geological Society, London. https://doi.org/10.1144/SP438.8

Pazzaglia, F. J. (2003), Landscape evolution models, *Development in Quaternary Science*, *1*, 247-274. https://doi.org/10.1016/S1571-0866(03)01012-1

Péron-Pinvidic, G., and G. Manatschal (2010), From microcontinents to extensional allochthons: witnesses of how continents rift and break apart?, *Petroleum Geoscience*, *16*(3), 189-197. https://doi.org/10.1144/1354-079309-903

Phethean, J. J. J., L. M. Kalnins, J. v. Hunen, P. G. Biffi, R. J. Davies, and K. J. W. McCaffrey (2016), Madagascar's escape from Africa: A high-resolution plate reconstruction for the Western Somali Basin and implications for supercontinent dispersal, *Geochemistry, Geophysics, Geosystems*, *17*(12), 5036-5055. https://doi.org/10.1002/2016GC006624

Phillips, T. B., C. A.-L. Jackson, R. E. Bell, O. B. Duffy, and H. Fossen (2016), Reactivation of intrabasement structures during rifting: A case study from offshore southern Norway, *Journal of Structural Geology*, *91*, 54-73. https://doi.org/10.1016/j.jsg.2016.08.008

Pollack, H. N., S. Hurter, and J. R. Johnson (1993), Heat Flow from the Earth's Interior: Analysis of the Global Data Set, *Reviews of Geophysics*, *31*(3), 267-280. https://doi.org/10.1029/93RG01249

Pubellier, M., C. Rangin, X. Le Pichon, and DOTMED Working Group (2005), *DOTSEA : deep offshore tectonics of South East Asia : a synthesis of deep marine data in Southeast Asia*, Société géologique de France, Paris.

Reclus, É. (1876), *The Earth. A descriptive history of the phenomena of the life of the Globe*, 2nd ed., Bickers and Son, Leicester Square, London.

Reeves, C. V. (2017), The development of the East African margin during Jurassic and Lower Cretaceous times: a perspective from global tectonics, *Petroleum Geoscience*, *24*, 41-56. https://doi.org/10.1144/petgeo2017-021

Reeves, C. V., J. Teasdale, and E. S. Mahanjane (2016), Insight into the Eastern Margin of Africa from a new tectonic model of the Indian Ocean, *Geological Society London Special Publications*, *431*. https://doi.org/10.1144/SP431.12

Riley, T. R., I. L. Millar, M. K. Watkeys, M. L. Curtis, P. T. Leat, M. B. Klausen, and C. M. Fanning (2004), U-Pb zircon (SHRIMP) ages for the Lebombo rhyolites, South Africa: refining the duration of Karoo volcanism, *Journal of the Geological Society, London*, *161*, 547-550. https://doi.org/10.1144/0016-764903-181

Roberts, E. M., P. M. O'Connor, M. D. Gottfried, N. Stevens, S. Kapalima, and S. Ngasala (2004), Revised stratigraphy and age of the Red Sandstone Group in the Rukwa Rift Basin, Tanzania, *Cretaceous Research*, *25*(5), 749-759. https://doi.org/0.1016/j.cretres.2004.06.007

Royer, J.-Y., J. G. Sclater, and D. T. Sandwell (1989), A preliminary tectonic fabric chart of the Indian Ocean, *Proceedings of the Indian Academy of Science (Earth and Planetary Science)*, *98*(1), 7-24. https://doi.org/10.1007/BF02880373

Royer, J.-Y., R. D. Müller, L. M. Gahagan, L. A. Lawver, C. L. Mayes, D. Nürnberg, and J. G. Sclater (1992), A global isochron chart, *University of Texas Institute for Geophysics Technical Report Rep. 117*, 38 pp, University of Texas Institute for Geophysics.

Ruotoistenmäki, T. (2008), Geophysical maps and petrophysical data of Mozambique, *Geological Survey of Finland, Special Paper*, *48*, 65-80,

Sandwell, D. T., and W. H. F. Smith (2009), Global marine gravity from retracked Geosat and ERS-1 altimetry: Ridge segmentation versus spreading rate, *Solid Earth*, *114*(B1). https://doi.org/10.1029/2008JB006008

Sandwell, D. T., R. D. Muller, W. H. F. Smith, E. Garcia, and R. Francis (2014), New global marine gravity model from CryoSat-2 and Jason-1 reveals buried tectonic structure, *Science*, *346*(6205), 65-67. https://doi.org/10.1126/science.1258213

Schoenberg, R., T. F. Nägler, E. Gnos, J. D. Kramers, and B. S. Kamber (2003), The source of the Great Dyke, ZImbabwe, and its tectonic significance: evidence from Re-Os isotopes, *The Journal of Geology*, *111*(5), 565-578. https://doi.org/10.1086/376766

Schuchert, C. (1910), Paleogeography of North America *Geological Society of America Bulletin*, *20*(1), 427-606. https://doi.org/10.1130/GSAB-20-427

Schuchert, C. (1928), The making of paleogeographic maps, *Leopoldina*, *4*(Amerikaband), 116-125,

Scrutton, R. A. (1978), Davie fracture zone and the movement of Madagascar, *Earth and Planetary Science Letters*, *39*(1), 84-88. https://doi.org/10.1016/0012-821X(78)90143-7

Şengör, A. M. C., N. Lom, and N. G. Sağdıç (2018), Tectonic inheritance, structure reactivation and lithospheric strength: the relevance of geological history, *Geological Society London Special Publications*, *470*, 105-136. https://doi.org/10.1144/SP470.8

Senkans, A., S. Leroy, E. d'Acremont, R. Castilla, and F. Despinois (2019), Polyphase rifting and break-up of the central Mozambique margin, *Marine and Petroleum Geology*, *100*, 412-433. https://doi.org/10.1016/j.marpetgeo.2018.10.035

Seton, M., et al. (2012), Global continental and ocean basin reconstructions since 200 Ma, *Earth-Science Reviews*, *113*, 212-270. https://doi.org/10.1016/j.earscirev.2012.03.002

Simkin, T., and L. Siebert (1994), Volcanoes of the World: an Illustrated Catalog of Holocene Volcanoes and their Eruptions, in *Global Volcanism Program Digital Information Series GVP-3*, http://volcano.si.edu/search_volcano.cfm

Smith, M., and P. Mosley (1993), Crustal heterogeneity and basement influence on the development of the Kenya Rift, East Africa, *Tectonics*, *12*(2), 591-606. https://doi.org/10.1029/92TC01710

Storey, M., J. J. Mahoney, and A. D. Saunders (1997), Cretaceous basalts in Madagascar and the transition between plume and continental lithosphere mantle sources, in *Large Igneous Provinces: Continental, Oceanic, and Planetary Flood Volcanism*, edited by J. J. Mahoney and M. F. Coffin, pp. 95-122, American Geophysical Union. https://doi.org/10.1029/GM100p0095

Strahler, A. N. (1964), Quantitative geomorphology of drainage basins and channel networks, in *Handbook of Applied Hydrology*, edited by V. T. Chow, pp. 4-39 - 34-76, McGraw Hill, New York,

Tobler, W. (1988), Resolution, resampling, and all that, in *Building Data Bases for Global Science: the proceedings of the International Geographical Union Global Database Planning Project, held at Tylney Hall, Hampshire, UK, 9-13 May 1988*, edited by H. Mounsey and R. Tomlinson, pp. 129-137, Taylor and Francis, London,

Tuck-Martin, A., J. Adam, and G. Eagles (2018), New Plate Kinematic Model and Tectono-stratigraphic History of the East African and West Madagascan Margins, *Basin Research*, *30*(6), 1118-1140. https://doi.org/10.1111/bre.12294

Tucker, G. E., and R. L. Slingerland (1994), Erosional dynamics, flexural isostasy, and long-lived escarpments: a numerical modeling study, *Journal of Geophysical Research*, *99*(B6), 12229-12243. https://doi.org/10.1029/94JB00320

USGS (2019), Earthquake Catalog, USGS, https://earthquake.usgs.gov/earthquakes/search/

USGS World Energy Assessment Team (2000), U.S. Geological survey world petroleum assessment 2000 - description and results, *U.S. Geological Survey Digital Data Series*, *DDS-60*, https://pubs.usgs.gov/dds/dds-060/

Van der Beek, P. A., and J. Braun (1998), Numerical modelling of landscape evolution on geological time-scales: a parameter analysis and comparison with the south-eastern highlands of Australia, *Basin Research*, *10*, 49-68. https://doi.org/10.1046/j.1365-2117.1998.00056.x

Wessel, P. (1997), Sizes and ages of seamounts using remote sensing: Implications for intraplate volcanism, *Science*, *277*, 802-805. https://doi.org/10.1126/science.277.5327.802

Whipple, K. X., and B. J. Meade (2004), Timescale of Orogen Response to Tectonic and Climatic Forcing, *EOS Transactions, AGU, Fall Meeting Supplement*, *85*(47), file:c://REFERENCES/pdfs/w/whipple_meade_2004.jpg

Whittaker, J. M., S. Williams, S. M. Masterton, J. C. Afonso, M. Seton, T. C. Landgrebe, M. F. Coffin, and D. Müller (2013), Interactions among plumes, mantle circulation and mid-ocean ridges, in *American Geophysical Union, Fall Meeting 2013*, edited, San Francisco, https://www.earthbyte.org/gplates-2-0-software-and-data-sets/#hotspots

Williams, S., J. M. Whittaker, and S. Mazur (2010), What can potential field data really tell us about Continent-Ocean transitions?, *ASEG Extended Abstracts*, *2010*(1). https://doi.org/10.1081/22020586.2010.12041933

Yang, Z., and W. P. Chen (2010), Earthquakes along the East African Rift System: A multiscale, system-wide perspective, *Journal of Geophysical Research. Solid Earth*, *115*(B12). https://doi.org/10.1029/2009JB006779

Ziegler, A. M., D. B. Rowley, A. L. Lottes, D. L. Sahagian, M. L. Hulver, and T. C. Gierlowski (1985), Paleogeographic interpretation: with an example from the Mid-Cretaceous, *Annual Review of Earth and Planetary Sciences*, *13*, 385-425. https://doi.org/10.1146/annurev.ea.13.050185.002125

Geochemistry, Geophysics, Geosystems

Supporting Information for

Reclus, a new Database for Investigating the Tectonics of the Earth: an Example from the East African Margin and Hinterland

P. J. Markwick[1,3], D. A. Paton[2], and E. J. Mortimer[3]

1 Knowing Earth Limited, West Yorkshire, U.K.

2 TectonKnow Limited, West Yorkshire, U.K

3 School of Earth and Environment, University of Leeds, Leeds, West Yorkshire, U.K.

Contents of this file

Additional Supporting Information (Files uploaded separately)

Dataset S1. Reclus databases for East Africa study area (zipped ArcGIS shapefile and layer file)

Introduction

This supporting information includes ArcGIS shapefiles extracted from the database for the extent shown and discussed in this paper. These are provided as .zip files containing all the files comprising each shapefile with a .lyr (ArcGIS layer) file that contains the symbology.

This text document provides detailed information about the attribution fields used for each database.

Text S1.2. Structural Elements Database Attribution

The Structural Elements database is a digital, global, spatial database built in ArcGIS storing the geometry, kinematics, and history of structural and tectonic features. These features define the structural framework and include the following line elements: faults (features with 'evidence' of displacement), lineaments (features that may be structural but with no clear offset or other evidence of motion), bedding (S0), folds, and foliation. All have been captured as lines (polylines in ArcGIS, ESRI, 2017). Polygonization of fault throws used in prospect evaluation, and other detailed structural analyses are beyond the resolution of this database.

The map symbology used for the Structural Elements Database is presented in the Supplementary Information in Markwick (2019).

Field Name	Alias	Format	Notes
FID	FID		Internally generated ESRI field
SHAPE	Shape	Polyline	Internally generated ESRI field
STRUCT_ID	Structure ID	Text (10)	This field provides the link to the activation table (not included in the version described in this paper)
S_ID	Symbol ID	Text (6)	The symbol code for different features relating to the default legend
DESCRIPT	Description	Text (254)	Description for SID
TYPE	Structural Element Type	Text (10) Dropdown	To quickly sort between different structural feature types for illustrating in different ways Fo = Fold F = Fault B = Bedding Fn = Foliation L= Lineament T = Tectonic
CLASS	Class	Text (1)	This is the fault class based on whether the fault cuts basement (2), is crust defining (1), cuts basin stratigraphy, not including the basement, (3) or surficial layers only (4)
NAME	Name	Text (254)	Name of feature
EXPRESSION	Outcrop or Subcrop	Text (10) Dropdown	Dropdown menu for with following options: **O** = **Outcrop** = feature has surface expression in Present Day **S** = **Subcrop** = feature has no surface expression in Present Day <BLANK> = not defined
ASSOC	Association	Text (254)	Name of the group of features to which this feature belongs
STATUS	Status	Text (25) Dropdown	Activity at time of map; default is the status for present day A = Active HA = Historically Active I = Inactive U = Unknown
ACTIVITY	Activity Notes	Text (254)	More information on activity status, including the source of information used

FA	First Appearance	Text (100)	The quoted first appearance age for the feature, e.g., "Ypresian", "Ar/Ar 100 Ma."
FA_MA	First Appearance (Ma)	Float (8,4)	Absolute age in millions of years of the first appearance of the feature
LA_ACT	Last Activity	Text (100)	The quoted age of the last activity
LA_ACT_MA	Last Activity (Ma)	Float (8,4)	Absolute age in millions of years of last documented activity
APPEAR	Appear	Float	Appearance age (in Ma) of a feature used in plate reconstruction programs
DISAPPEAR	Disappear	Float	Disappearance age (in Ma) of the feature. In most cases, this will be "Future" (in gPlates terminology, https://www.gplates.org/) or "-9999" in PGAP terminology
AGE_CONFID	Dating Confidence	Text (50) Dropdown menu	A value between 0 (lowest) and 5 (highest). See Table S6 for details
DATING	Dating method	Text (50) Dating method used for age assignments. Dropdown menu	The principal dating methodology that was used for the age assignments. Ar/Ar K/Ar Fission Track Other radiometric Magnetostratigraphy Biostratigraphy Geological Inference Secondary information Estimated
AGE_NOTES	Age Dating Notes	Text (254)	Notes related to the age dating
MAP_CONFID	Mapping Confidence	Text (50) Dropdown menu	A value between 0 (lowest) and 5 (highest). See Table S6 for details
COMP_SCALE	Compilation Scale	Long Dropdown menu	Dropdown menu for the approximate scale at which the feature was captured: 10000000 5000000 2000000 1000000 750000 500000 250000 100000 50000 10000
EXPLAN	Explanation	Text (254)	Explanation of the basis for the mapped feature as recorded
GEOL_NOTES	Geological Notes	Text (254)	Geological notes related to the feature
INPUT_DATA	Input Data	Text (254)	List summary of the key inputs from: Gravity Magnetics Radar Literature Landsat Fieldwork Geology Map Personal Communication

COMPILER	Compiler	Text (254)	Name of the compiler(s) e.g. "PJM (May 2017), ed PJM (Jun 2017)"
REF_CIT01	Reference 1	Text (150)	The reference citation accessed through a reference ID in the working database and related reference database. In this SI we have only included those reference fields with at least one value.
REF_CIT02	Reference 2	Text (150)	
REF_CIT03	Reference 3	Text (150)	
REF_CIT04	Reference 4	Text (150)	
REF_CIT05	Reference 5	Text (150)	

Table S1. Attribution fields for the Structural Elements database. Citations in the final database replace reference IDs.

Text S1.2 Crustal Facies Database Attribution

The Crustal Facies Database describes the geometry and composition of the Earth's crust. The crustal facies define the crustal architecture with the structural framework (here recorded as the Structural Elements Database).

The map symbology used for the Crustal Facies Database is that presented in this paper.

Field Name	Alias	Format	Notes
FID	FID		Internally generated ESRI field
SHAPE	Shape	Polygon	Internally generated ESRI field
SYM_ID	Symbol ID	Text (6)	The symbol code for different features relating to the default legend
DESCRIPT	Description	Text (254)	The description relating to the symbol code in the legend
NAME	Name	Text (254)	Name of feature
ASSOC	Association	Text (254)	Name of a group of features to which this feature belongs
ASSEMB_ID	Facies Assemblage ID	Text (6)	The traditional facies assemblage definition
ASSEMB	Facies Assemblage	Text (20) Dropdown	The traditional facies assemblage definition Continental Oceanic Collisional Extensional Strike-slip Transitional
MANAT_ID	Manatschal Classification ID	Text (6)	The ID is used to symbolize polygons using the crustal classification used by Manatschal and co-workers (Péron-Pinvidic and Manatschal, 2010).
MANAT	Manatschal Classification	Text (50) Dropdown	The crustal classification used by Manatschal and co-workers (Péron-Pinvidic and Manatschal, 2010). Proximal (stretching) Necking (thinning) Distal (hyper-extension) Outer (exhumation-oceanization)
MAP_ABB	Map Abbreviation	Text (30)	CONTINENTAL Ci = continental indet. Ctk = thick continental, >40 km C = continental, 30-40 km Cth = thin continental, 10-30 km Cvth = very thin continental, <10 km Ci_{cra} = craton indet. Ctk_{cra} = thick craton, >40 km C_{cra} = craton, 30-40 km Ctn_{cra} = thin craton, 10-30 km Cth_{cra} = very thin craton, <10 km Ci_{arc} = continental arc indet. Cth_{arc} = thick continental arc, >40 km C_{arc} = continental arc, 30-40 km

			Ctn_{arc} = thin continental arc, 10-30 km $Cvtn_{arc}$ = very thin continental arc, <10 km Ci_{mob} = mobile belt indet. Ctk_{mob} = thick mobile belt, >40 km C_{mob} = mobile belt, 30-40 km Ctn_{mob} = thin mobile belt, 10-30 km $Cvtn_{mob}$ = very thin mobile belt, <10 km Ci_{acc} = accreted complex indet. Ctk_{acc} = thick accreted complex, >40 km C_{acc} = accreted complex, 30-40 km Ctn_{acc} = thin accreted complex, 10-30 km Ctn_{acc} = very thin accreted complex, <10 km Ci_{oc} = oceanic arc indet. Ctk_{oc} = thick oceanic arc, >40 km C_{oc} = oceanic arc, 30-40 km Ctn_{oc} = thin oceanic arc, 10-30 km $Cvth_{oc}$ = very thin oceanic arc, <10 km MAGMATIC ADDITION Ci_{mg} = mixed continental crust indet. Ctk_{mg} = thick mixed continental crust, >40 km C_{mg} = mixed continental crust, 30-40 km Cth_{mg} = thin mixed continental crust, 10-30 km $Cvth_{mg}$ = very thin mixed continental crust, <10 km M_{mg} = mantle magmatic additoin Oi = Oceanic indet Ovtk = Very thick oceanic, >20 km Otk = Thick oceanic, 7-20 km O = (Typical) oceanic, 5-7 km Otn = thin oceanic, <5 km M = mantle M_{sp} = sepentinized mantle
PLATEID	Plate ID	Short Integer	Plate ID needs to be compatible with gPlates and PaleoGIS formats
PLATE_NAME	Plate Name	Text (254)	The name of the tectonic plate.
FA	First Appearance	Text (100)	The quoted first appearance age for the feature, e.g., "Ypresian", "Ar/Ar 100 Ma"
FA_MA	First Appearance (Ma)	Float (8,4)	Absolute age in millions of years of the first appearance of the feature
APPEAR	Appear	Float	Appearance age (in Ma) of a feature used in plate reconstruction programs
DISAPPEAR	Disappear	Float	Disappearance age (in Ma) of the feature. In most cases, this will be "Future" (in gPlates terminology, https://www.gplates.org/) or "-9999" in PGAP terminology
AGE_CONFID	Dating Confidence	Text (50) Dropdown menu	A value between 0 (lowest) and 5 (highest). See Table S6 for details
DATING	Dating method	Text (50)	The principal dating methodology that is used for the age assignments. A = Ar/Ar

		Dating method used for age assignments. Dropdown menu	K = K/Ar F = Fission Track O = Other radiometric M = Magnetostratigraphy B = Biostratigraphy G = Geological Inference S = Secondary information E = Estimated
AGE_NOTES	Age Dating Notes	Text (254)	Notes related to the age dating
MAP_CONFID	Mapping Confidence	Text (50) Dropdown menu	A value between 0 (lowest) and 5 (highest). See Table S6 for details
COMP_SCALE	Compilation Scale	Long Dropdown menu	Dropdown menu for the approximate scale at which the feature was captured: 10000000 5000000 2000000 1000000 750000 500000 250000 100000 50000 10000
EXPLAN	Explanation	Text (254)	Explanation of the mapping. Information on the basis for the definition of the feature
GEOL_NOTES	Geological Notes	Text (254)	Geological notes related to the feature
INPUT_DATA	Input Data	Text (254)	List summary of key inputs from: Gravity Magnetics Radar Literature Landsat Fieldwork Geology Map Personal Communication
COMPILER	Compiler	Text (254)	Name of the compiler(s) e.g. "PJM (May 2017), ed PJM (Jun 2017)"
REF_CIT01	Reference 1	Text (150)	The reference citation accessed through a reference ID in the working database and related reference database. In this SI we have only included those reference fields with at least one value.
REF_CIT02	Reference 2	Text (150)	
REF_CIT03	Reference 3	Text (150)	
REF_CIT04	Reference 4	Text (150)	
REF_CIT05	Reference 5	Text (150)	
REF_CIT06	Reference 6	Text (150)	
REF_CIT07	Reference 7	Text (150)	
REF_CIT08	Reference 8	Text (150)	

Table S1.2. Attribution fields for the Crustal Facies database. Reference IDs are replaced by citations in the final database.

Text S1.3 Igneous Features Database Attribution

The Igneous Features database is a digital, global, spatial database showing the geometry, age and composition of intrusive and extrusive rocks around the world.

The map symbology used for the Igneous Features Database is that presented in the Supplementary Information in Markwick (2019).

Field Name	Alias	Format	Notes
FID	FID		Internally generated ESRI field
SHAPE	Shape	Polyline	Internally generated ESRI field
IG_ID	Symbol ID	Text (6)	The symbol code for different features relating to the default legend: IG300 = Igneous indeterminate IG310 = Igneous extrusive IG320 = Igneous intrusive
DESCRIPT	Description	Text (254)	The description relating to the symbol code in the legend
IG_FORM	Igneous Form	Text (590 Dropdown	EXTRUSIONS Continental Flood Basalt Oceanic Flood Basalt Seaward dipping reflectors Shield Volcano Strato Volcano Cinder Cone Caldera Crater Lava Dome Fissure Vent Seamount Submarine Ridge Submarine Plateau Volcanic Field Lava Flow Pyroclastics, undiff. Pyroclastic flow Volcanic Ash Sub-volcanic INTRUSIONS Dyke Dyke Swarm Sill Batholith Stock Laccolith Lopolith Ring Complex Intrusion indet. MIXED

			Large Igneous Province indet. Silicic Large Igneous Province indet. Indeterminate Igneous Complex
MAP_ABB	Map Abbreviation	Text (30)	EXTRUSIONS e-CFB = Continental Flood Basalt e-OFB = Oceanic Flood Basalt e-SDR = Seaward dipping reflectors e-ShV = Shield Volcano e-StV = Strato Volcano e-CC = Cinder Cone e-Cld = Caldera e-Cra = Crater e-LD = Lava Dome e-FV = Fissure Vent e-SMT = Seamount e-SR = Submarine Ridge e-SP = Submarine Plateau e-ind = Extrusion indet. e-VF = Volcanic Field e-LF = Lava Flow e-Py = Pyroclastics, undiff. e-PyF = Pyroclastic flow e-Ash = Volcanic Ash sV = Sub-volcanic INTRUSIONS i-D = Dyke i-DS = Dyke Swarm i-S = Sill i-B = Batholith i-Bs = Stock i-Lac = Laccolith i-Lop = Lopolith i-RC = Ring Complex i-ind = Intrusion indet. MIXED LIP = Large Igneous Province indet. sLIP = Silicic Large Igneous Province indet. Ig = Indeterminate IgC = Igneous Complex
NAME	Name	Text (254)	Name of feature
ASSOC	Association	Text (254)	Name of a group of features to which this feature belongs
EXPRESSION	Outcrop or Subcrop	Text (10) Dropdown	Dropdown menu for with following options: O = Outcrop the feature has surface expression in Present Day S = Subcrop the feature has no surface expression in Present Day <BLANK> not defined
SETTING	Tectonic setting	Text (50) Dropdown	Tectonic setting of the igneous feature at the time of formation: C = Continental

			O = Oceanic COT = Continent-Ocean Transition Zone I = Indeterminate M = Mixed
TM_ID	Thermo-mechanical Symbol ID	Text (6)	Symbol ID for principal last thermo-mechanical event
TM_DESC	Thermo-mechanical Description	Text (254)	Description of principal last Thermo-mechanical event to affect the area
TM_ABB	Thermo-mechanical Abbreviation	Text (5)	Abbreviation for map (rather than write in the whole description on map)
LITH_ID	Lith Symbol ID	Text (6)	Symbol ID for principal lithology
LITH_DESC	Lithological Description	Text (254)	Description of principal lithology
LITHS	Petrology	Text (254)	Rock types comprising the igneous feature written in full (basically lithology notes)
VOL_MIN	Minimum volume (km3)	Double	Minimum volume in km^3 as cited by references
VOL_MAX	Maximum volume (km3)	Double	Maximum volume in km^3 as cited by references
FA_ACT	Start of Activity	Text (100)	The quoted first activity age for the feature, e.g., "Ypresian," "Ar/Ar 100 Ma."
LA_ACT	End of Activity	Text (100)	The quoted last activity age for the feature, e.g., "Ypresian", "Ar/Ar 100 Ma."
FA_ACT_MA	Age of start of the activity (Ma)	Float (8,4)	Absolute age in millions of years
LA_ACT_MA	Age of end of the activity (Ma)	Float (8,4)	Absolute age in millions of years
DURATION_MA	Duration of activity	Float (8,4)	Absolute age in millions of years
APPEAR	Appear	Float	Appearance age (in Ma) of a feature used in plate reconstruction programs
DISAPPEAR	Disappear	Float	Disappearance age (in Ma) of the feature. In most cases, this will be "Future" (in gPlates terminology, https://www.gplates.org/) or "-9999" in PGAP terminology
AGE_CONFID	Dating Confidence	Text (50) Dropdown menu	A value between 0 (lowest) and 5 (highest). See Table S6 for details.
DATING	Dating method	Text (50) Dating method used for age assignments. Dropdown menu	The principal dating methodology that is used for the age assignments. A = Ar/Ar K = K/Ar F = Fission Track O = Other radiometric M = Magnetostratigraphy B = Biostratigraphy G = Geological Inference S = Secondary information E = Estimated
AGE_NOTES	Age Dating Notes	Text (254)	Notes related to the age dating
MAP_CONFID	Mapping Confidence	Text (50) Dropdown menu	A value between 0 (lowest) and 5 (highest). See Table S6 for details

COMP_SCALE	Compilation Scale	Long Dropdown menu	Dropdown menu for the approximate scale at which the feature was captured: 10000000 5000000 2000000 1000000 750000 500000 250000 100000 50000 10000
EXPLAN	Explanation	Text (254)	Explanation of the mapping. Information on the basis for the definition of the feature
GEOL_NOTES	Geological Notes	Text (254)	Geological notes related to the feature
INPUT_DATA	Input Data	Text (254)	List summary of key inputs from: Gravity Magnetics Radar Literature Landsat Fieldwork Geology Map Personal Communication
COMPILER	Compiler	Text (254)	Name of the compiler(s), e.g., "PJM (May 2017), ed PJM (Jun 2017)."
ADMIN	Compiler notes	Text (254)	Compiler comments related to the feature for record
REF_CIT01	Reference 1	Text (150)	The reference citation accessed through a reference ID in the working database and related reference database. In this SI we have only included those reference fields with at least one value.
REF_CIT02	Reference 2	Text (150)	
REF_CIT03	Reference 3	Text (150)	
REF_CIT04	Reference 4	Text (150)	
REF_CIT05	Reference 5	Text (150)	
REF_CIT06	Reference 6	Text (150)	
REF_CIT07	Reference 7	Text (150)	
REF_CIT08	Reference 8	Text (150)	

Table S1.3. Attribution fields for the Igneous Features database. Reference IDs are replaced by citations in the final database.

Text S1.4 Geodynamics Database Attribution

The Geodynamics databases are digital, global databases showing the geometry and nature of the last thermo-mechanical event to affect the Earth's lithosphere. The default database (this paper) shows the present-day geodynamic state. This provides analogs and the basis for investigating the interaction of geodynamics with crustal architecture and landscape dynamics. Databases are also constructed for each timeslice mapped (paleogeography).

These databases are designed to provide the information needed for modeling basin evolution, plate kinematics, paleogeographic reconstruction, and paleolandscape dynamics.

The (present-day) Geodynamics Database inherits from both the Structural Elements and Crustal Facies database. In many cases, the extent of the effects of a geodynamic action is defined by the limits of a crustal block. However, the exact spatial limits of geodynamics are not always clear. The interaction of geodynamics on the crustal type and structural framework dictates basin development and geometry, accommodation space, and uplift. The result is the paleolandscape (paleogeography) at a particular time and place.

The map symbology used for the Geodynamics Database is presented in the Supplementary Information in Markwick (2019).

Field Name	Alias	Format	Notes
FID	FID		Internally generated ESRI field
SHAPE	Shape	Polygon	Internally generated ESRI field
TM_ID	Symbol ID	Text (6)	Symbol ID for principal last thermo-mechanical event
DESCRIPT	Description	Text (254)	The description relating to the symbol code in the legend
NAME	Name	Text (254)	Name of feature
ASSOC	Association	Text (254)	Name of a group of features to which this feature belongs
STRESS	Dominant Stress	Text (10) Dropdown Menu	C = Compression E = Extension V = Vertical U = Unknown
TM	Tectonics	Text (50) Dropdown Menu	The mapped thermo-mechanical process as it relates to tectonics. This is more specific and subdivides the different extensional and compressional processes. These sub-divisions can result in a different expression in the crust and thereby the resulting landscape. A = Anorogenic C = Compression, undiff CC = Continent-Continent, undiff. CCtk = Continent-Continent, thick-skinned CCtn = Continent-Continent, thin-skinned CO = Continent-Ocean, undiff. COtk = Continent-Ocean, thick-skinned COtn = Continent-Ocean, thin-skinned OO = Ocean-Ocean, undiff.

			TP = Transpressional E = Extension, undiff. TT = Transtensional V = Vertical, undiff. F = Flexure, undiff. I = Isostatic, undiff. Volc = Volcanic, undiff. M = Mantle, undiff. S = Sag
MAP_ABB	Map Abbreviation	Text (30) Dropdown Menu	The abbreviation for mapping (rather than write in whole description on map) A = Anorogenic C = Compression, undiff C-C = Continent-Continent, undiff. C-Cthick = Continent-Continent, thick-skinned C-Cthin = Continent-Continent, thin-skinned C-O = Continent-Ocean, undiff. C-Othick = Continent-Ocean, thick-skinned C-Othin = Continent-Ocean, thin-skinned O-O = Ocean-Ocean, undiff. TP = Transpressional Ext = Extension, undiff. TT = Transtensional V = Vertical, undiff. Fx = Flexure, undiff. Iso = Isostatic, undiff. Volc = Volcanic, undiff. M = Mantle, undiff. S = Sag
TOP_AGE	Top Age	Text (100)	The quoted chronostratigraphic age as text
BTM_AGE	Bottom Age	Text (100)	The quoted chronostratigraphic age as text
AGE_RANGE	Age Range	Text (254)	The quoted chronostratigraphic range as text
TOP_AGE_MA	Top Age (Ma)	Double	Age in millions of years based on timescale used
BTM_AGE_MA	Bottom Age (Ma)	Double	Age in millions of years based on timescale used
APPEAR	Appear	Float	Appearance age (in Ma) of a feature used in plate reconstruction programs
DISAPPEAR	Disappear	Float	Disappearance age (in Ma) of the feature. In most cases this will be "Future" (in gPlates terminology, https://www.gplates.org/) or "-9999" in PGAP terminology
AGE_CONFID	Dating Confidence	Text (50) Dropdown menu	A value between 0 (lowest) and 5 (highest). See Table S6 for details.
DATING	Dating method	Text (50) Dating method used for age assignments Dropdown menu	The principal dating methodology that is used for the age assignments A = Ar/Ar K = K/Ar F = Fission Track O = Other radiometric M = Magnetostratigraphy B = Biostratigraphy G = Geological Inference S = Secondary information E = Estimated
AGE_NOTES	Age Dating Notes	Text (254)	Notes related to the age dating

MAP_CONFID	Mapping Confidence	Text (50) Dropdown menu	A value between 0 (lowest) and 5 (highest). See Table S6 for details.
COMP_SCALE	Compilation Scale	Long Dropdown menu	Dropdown menu for the approximate scale at which the feature was captured: 10000000 5000000 2000000 1000000 750000 500000 250000 100000 50000 10000
EXPLAN	Explanation	Text (254)	Explanation of the mapping. Information on the basis for the definition of the feature
GEOL_NOTES	Geological Notes	Text (254)	Geological notes related to the feature
INPUT_DATA	Input Data	Text (254)	List summary of key inputs from: Gravity Magnetics Radar Literature Landsat Fieldwork Geology Map Personal Communication
COMPILER	Compiler	Text (254)	Name of the compiler(s) e.g. "PJM (May 2017), ed PJM (Jun 2017)."
REF_CIT01	Reference 1	Text (150)	The reference citation accessed through a reference ID in the working database and related reference database. In this SI we have only included those reference fields with at least one value.
REF_CIT02	Reference 2	Text (150)	
REF_CIT03	Reference 3	Text (150)	
REF_CIT04	Reference 4	Text (150)	
REF_CIT05	Reference 5	Text (150)	
REF_CIT06	Reference 6	Text (150)	
REF_CIT07	Reference 7	Text (150)	

Table S1.4. Attribution fields for the Geodynamics database. Citations in the final database replace reference IDs.

Code	Summary	Age dating confidence	Mapping confidence
5	No changes expected	Multiple lines of information converging on precise dates (very high temporal resolution)	The geometry, position, and geological description are constrained by multiple primary evidence supported by geological data in reputable publications. All lines of evidence are consistent. Polygon features constrained by a high density of data
4	Minor changes possible	Good biostratigraphic control and/or radiometric ages (high temporal resolution)	The geometry, position, and geological description are constrained by multiple lines of primary evidence and a good spread of data, supported by geological data in reputable publications. But interpretations are equivocal. Minor changes in geometry are possible with more data.
3	Changes probable	Some biostratigraphic control (low temporal resolution); correlation from an area with more precise, high confidence, information	The feature is identified and interpreted from limited primary sources, supported by other published data, but the data spread is limited, and interpretations are equivocal. Changes probable with more lines of evidence, especially consideration of higher resolution primary data and model testing. e.g., features based on only potential fields data to constrain boundaries, which are not as highly resolvable as those through seismic, Landsat, or field observations.
2	Changes expected	Geological inference: stratigraphic relationships (e.g., onlapping, cross-cutting relationships) with dated rocks;	Interpretations from secondary source(s) with references supporting primary data (but not seen). The geological interpretation is equivocal or limited to one source. Geological interpretations may be generalized or absent, e.g., no information on kinematics for structural features. The feature requires testing against primary data.
1	Revision and testing required	Secondary information: age from publication but without explanation of methods used	Feature captured from a single secondary source with no supporting information as to why and no evidence in primary data. e.g., information is taken directly from an image in a paper but has not been checked against other data and is without supporting data.
0	Revision and testing essential	Source unknown	Source unknown. The feature is unchecked with no constraining secondary or primary information. e.g., a feature based on an image found on the internet or anecdotal.

Table S1.5. Confidence scheme used in the databases with explanations.

Data Set S1. Reclus databases for East Africa study area (zipped ArcGIS shapefile and layer file)

DS S1 contains shapefiles extracted for the AOI from the Reclus databases of Structural Elements, Crustal Facies, Igneous Features (lines and polygons), Geodynamics. For each shapefile, we have provided a .lyr (layer) file which includes the default symbology.